Tracing devastating fires in Portugal to a snow archive in the Swiss Alps: a case study

Dimitri Osmont[1,2,3,a], Sandra Brugger[3,4,*], Anina Gilgen[5,*], Helga Weber[3,6,*], Michael Sigl[1,3], Robin L. Modini[7], Christoph Schwörer[3,4], Willy Tinner[3,4], Stefan Wunderle[3,6], Margit Schwikowski[1,2,3]

[1]Laboratory of Environmental Chemistry, Paul Scherrer Institut, 5232 Villigen, Switzerland
[2]Department of Chemistry and Biochemistry, University of Bern, 3012 Bern, Switzerland
[3]Oeschger Centre for Climate Change Research, University of Bern, 3012 Bern, Switzerland
[4]Institute of Plant Sciences, University of Bern, 3012 Bern, Switzerland
[5]Institute for Atmospheric and Climate Science, ETH Zürich, 8092 Zürich, Switzerland
[6]Institute of Geography, University of Bern, 3012 Bern, Switzerland
[7]Laboratory of Atmospheric Chemistry, Paul Scherrer Institut, 5232 Villigen, Switzerland
*These authors equally contributed to this work.
[a]Now at Institut des Géosciences de l'Environnement, Université Grenoble-Alpes, 38400 Saint Martin d'Hères, France

Correspondence to: Margit Schwikowski (margit.schwikowski@psi.ch)

Abstract. Recent large wildfires, such as those in Portugal in 2017, have devastating impacts on societies, economy, ecosystems and environments. However, wildfires are a natural phenomenon, which has been exacerbated by land use during the past millennia. Ice cores are one of the archives preserving information on fire occurrences over these timescales. A difficulty is that emission sensitivity of ice cores is often unknown, which constitutes a source of uncertainty in the interpretation of such archives. Information from specific and well-documented case studies is therefore useful to better understand the spatial representation of ice-core burning records. The wildfires near Pedrógão Grande in Central Portugal in 2017 provided a test bed to link a fire event to its footprint left in a high-alpine snowpack considered a surrogate for high-alpine ice-core sites. Here, we (1) analyzed black carbon (BC) and microscopic charcoal particles deposited in the snowpack close to the high-alpine research station Jungfraujoch in the Swiss Alps, (2) calculated backward trajectories based on ERA-Interim reanalysis data and simulated the transport of these carbonaceous particles using a global aerosol-climate model, and (3) analyzed the fire spread, its spatial and temporal extent, as well as its intensity, with remote sensing (e.g. MODIS) active fire and burned area products. According to modelled emissions of the FINN v1.6 database, the fire emitted a total amount of 203.5 tons BC from a total burned area of 501 km^2 as observed on the basis of satellite fire products. Backward trajectories unambiguously linked ~~A~~a peak of atmospheric equivalent BC ~~(~~eBC~~)~~ observed at the Jungfraujoch research station on 22nd June, with elevated ~~e~~BC ~~-~~levels until the 25th June, with the highly intensive fires in Portugal. The atmospheric signal~~,~~ is in correspondence with an outstanding peak in ~~refractory BC (rBC) and~~ microscopic charcoal observed in the snow layer, depositing nearly as many charcoal particles as during an average year in other ice archives. In contrast to charcoal, the amount of atmospheric BC deposited during the fire episode was minor due to a lack of precipitation. Simulations with a global aerosol climate model supported that the observed microscopic charcoal particles originated from the fires in Portugal and that their contribution to the BC signal in snow was negligible. ~~rBC was mainly scavenged by wet deposition and we obtained~~

scavenging ratios ranging from 81 to 91. Unlike for microscopic charcoal, the model did not well reproduce the observed rBC signal. Our study revealeds that microscopic charcoal can be transported over long distances (1500 km), and that snow and ice archives are much more sensitive to distant events than sedimentary archives, for which the signal is dominated by local fires. Microscopic charcoal concentrations were exceptionally high since this single outstanding event deposited as many charcoal particles per day as during an average year in ice cores. This study unambiguously links the fire tracers in the snow with the highly intensive fires in Portugal, where a total burned area of 501 km^2 was observed on the basis of satellite fire products. According to our simulations, this fire event emitted at least 203.5 tons of BC.The findings are important for future ice-core studies, as they document that for BC as fire tracer the signal preservation depends on precipitation. Single events, like this example, might not be preserved due to unfavorable meteorological conditions.

1 Introduction

Fires are an important component of terrestrial ecosystems as they substantially control vegetation cover and contribute to the global carbon budget (e.g. Bond et al., 2005; Hantson et al., 2015). Global CO_2 emissions from fires, including landscape and biomass (i.e. biomass combustion from domestic and industrial uses), represent around 50% of those produced by fossil fuel burning (Bowmann et al., 2009). Current global CO_2 emissions from fires, including landscape and biomass, represent around 50 % of the global CO_2 emissions produced by fossil fuel burning (Bowman et al., 2009). Fires exert an influence on the climate system as they emit greenhouse gases and aerosols (Andreae and Merlet, 2001) and change surface albedo (Randerson et al., 2006), as well as on vegetation and soil carbon (Page et al., 2002). In the last two decades, the occurrence of devastating wildfires has increased in many regions of the world, leading to substantial socioeconomic and environmental consequences (Moritz et al., 2014). In the context of global warming, fire risk (Pechony et al., 2010), frequency (Keywood et al., 2013), and season severity (Flannigan et al., 2013) are potentially increasing with significant feedbacks on terrestrial and atmospheric systems (Bowman et al., 2011). To understand these future impacts, paleofire reconstructions provide an important tool for assessing long-term changes in past fire activity and can help to disentangle the influence of climate and humans on biomass burning. Most of the currently available sedimentary records have large chronological uncertainties in the youngest part of the records (Marlon et al., 2016) and reflect small local to regional catchments (Adolf et al., 2018). To address global fire activity trends, ice cores from polar (see e.g. Arienzo et al., 2017; Fischer et al., 2015; Keegan et al., 2014; Legrand et al., 1992; Legrand and De Angelis, 1996, Legrand et al., 2016; Whitlow et al., 1994; Zennaro et al., 2014) and high-altitude glaciers (see e.g. Brugger et al., 2018a, 2019a; Eichler et al., 2011; Osmont et al., 2018, 2019; Yalcin et al., 2006) have a high potential since they record fire activity from regional to continental scales and usually provide well-constrained chronologies (see e.g. Herren et al., 2013; Konrad et al., 2013; Uglietti et al., 2016).

Fires emit a wide range of chemical compounds and particles to the atmosphere, such as black carbon (BC) and charcoal. If transported over long distances, these particles can be deposited with precipitation or by gravitational settling on the snowpack, where they will be archived, and can be subsequently retrieved by ice-core drilling. However, ice-core catchment areas are not

often precisely known due to a lack of information about emission, transport and deposition processes. Case studies are essential to understand these processes including fire extent, fuel load, plume transport, biomass burning tracer deposition and preservation in the snowpack (e.g. Kaspari et al., 2015). Modelling of fire tracers (e.g. BC or charcoal) from the fire source to the deposition site provides a direct link and quantification of the archived biomass burning tracers. Detailed information to quantify the amount, frequency and intensity of biomass burning emissions relies mainly on satellite observations (e.g. occurrence of active fires, fire radiative power (i.e. intensity; FRP), burned area and vegetation cover). A limiting factor is the availability of long-term satellite products with sufficient temporal and spatial resolution. Recently, an active fire product was developed for Europe reaching back until 1985 (see Weber and Wunderle, 2019). Therefore, a direct linkage between specific fire events and ice core observations is very challenging, especially for biomass burning events that occurred some decades or centuries ago. Thus, the fire footprint of ice-core sites and the preservation of single biomass burning events in these archives remain largely unknown. Pioneer case studies have shown that elevated concentrations of ammonium, potassium and formate in Greenland's atmosphere and snow could be directly linked to forest fires in Canada (Dibb et al., 1996). More recent case studies confirmed that BC emissions from fires can be preserved in snow and ice archives at sub-continental scales. For instance, BC peaks in Greenland snowpits were associated with specific biomass burning events in Canada with the help of remote sensing and modelling tools (Thomas et al., 2017). BC emissions from the oil well fires in Kuwait in 1991 during the Gulf War were detected unambiguously in an ice core from Muztagh Ata, Northern Tibet (Zhou et al., 2018). However, for Europe, characterized by highly fragmented landscapes and smaller mean burned area compared to other continents (Mouillot and Field, 2005), specific case studies are missing.

Here, we focus on an outstanding wildfire event starting on 17th June 2017 in Portugal. Portugal was affected by a severe heat wave with temperatures above 40 °C in June 2017 and during a dry thunderstorm, lightning ignited the forests dominated by non-native *Eucalyptus* plantations near Pedrógão Grande in Central Portugal (Fig. 1). The highly flammable vegetation resulted in a rapid and uncontrolled spread of the fire with devastating impacts, leading to the worst death toll Portugal ever experienced for a fire. 64 people lost their life and 254 were injured (Gómez-González et al., 2018) until the fires were finally extinguished on 24th June. A large plume of smoke was emitted and transported to the northeast from the burning site. On 21st June, the automatic lidar operated by MeteoSwiss (Federal Office of Meteorology and Climatology, Switzerland) in Payerne, Switzerland, detected a layer of smoke between 3000 and 5000 m a.s.l. corresponding to the arrival of the plume. The signal intensified on 22nd June and its Portuguese origin was confirmed by atmospheric backward trajectory analysis (MeteoSwiss, 2017). The smoke layer became visible in the morning hours of 22nd June on the Jungfraujoch (JFJ) research station webcam, located at 3580 m a.s.l. in the Bernese Alps. At the same time, a peak in atmospheric equivalent black carbon (eBC) ~~, following the terminology recommendations by Petzold et al., 2013)~~ was detected by the Multi-Angle Absorption Photometer (MAAP, optical method for BC quantification, Petzold and Schönlinner, 2004) installed at the research station (Fig. 2a). The term eBC is used for black carbon data derived from optical absorption methods, together with a suitable mass absorption cross-section (MAC) for the conversion of light absorption coefficient into mass concentration (Petzold et al., 2013). Elevated eBC values lasted until 25th June when the first snowfall after the event occurred.

The exceptional conditions of this Portuguese fire event producing a plume that was recorded unambiguously at the high-alpine research station JFJ in Switzerland, located close to perennial snow archives, provided an ideal situation to analyze in detail the processes related to emission, transport and deposition of fire tracers in a high-mountain snowpack. ~~Several well-studied ice cores were already collected in the vicinity, namely from Fiescherhorn glacier and Colle Gnifetti, which are located 6 km east and 70 km south, respectively (Jenk et al., 2006; Sigl et al. 2018).~~

2 Methods

2.1 Study site and meteorological conditions

The high-altitude research station Jungfraujoch (46°32´ N 7°59´ E, Fig. 1) is located on the ~~eponymous~~ pass between the summits of Jungfrau and Mönch in the Bernese Alps. Built at an altitude of 3580 m a.s.l., the surrounding high-alpine environment is characterized by glaciers and cliffs. The north side, facing the Swiss Plateau, consists of a steep ice fall while the relatively flat south slopes host the large Jungfraufirn glacier feeding the Aletsch glacier. The JFJ site lies only partially within the free troposphere, being frequently influenced by uplifted air from the planetary boundary layer (e.g. Baltensperger et al., 1997; Bukowiecki et al., 2016). Aerosol monitoring at JFJ provides continuous long-term atmospheric records of many parameters including eBC concentration. In addition, a weather station provides meteorological data, but precipitation is not monitored at JFJ due to the difficulty of obtaining accurate data as most precipitation occurs in form of snow in frequent association with strong winds. The closest precipitation data available is from the automatic weather station Itramen (2162 m a.s.l.), operated by the Institute for Snow and Avalanche Research (WSL-SLF) and located 9 km to the northwest of JFJ. Following the Portugal fires, precipitation (rainfall) was recorded at Itramen on 25th, 26th, 27th, 28th and 29th June, bringing 32, 42.8, 2.0, 49.6 and 35.2 mm of water, respectively (data from SLF © 2019, SLF). We used the JFJ webcam to determine whether snowfall occurred at the same time at JFJ, which was the case except for 27th June.

2.2 Snowpit and sampling

A snowpit was collected on 30th June 2017, around 20 m off the prepared trail between JFJ and Mönchsjochhütte and 400 m east from the Jungfraujoch tunnel exit onto the glacier, at an altitude of 3460 m a.s.l. A massive ice layer prevented us from digging deeper than 1.10 m. Density was measured on the spot for each layer, by weighing a stainless steel cylinder of known volume filled with snow. Following the stratigraphic study, 20 samples were collected at about 5 cm resolution by pushing pre-cleaned 50-mL polypropylene vials vertically in the snow wall. Ice layers were sampled specifically (if thick enough) to check the potential impact of melting on the chemical composition of the snowpack. 20 replicate samples were retrieved at the same resolution to test the reproducibility of the experiment. In addition, 6 pre-cleaned 1-L PETG jars were filled with 0.2 to 0.5 kg snow for microscopic charcoal analysis, at 10 cm resolution between 20 and 80 cm depth.

2.3 Analytical methods

Samples were stored in frozen state and were melted just before analysis of refractory BC (rBC) and major ions at the Paul Scherrer Institute. rBC stands for black carbon measured by incandescence methods (Petzold et al., 2013) and analysis followed the method described by Wendl et al. (2014): after sample melting at room temperature and a 25-min sonication in a ultrasonic bath, rBC was quantified using a Single Particle Soot Photometer (SP2, Droplet Measurement Technologies, USA, Schwarz et al., 2006; Stephens et al., 2003) coupled to an APEX-Q jet nebulizer (Elemental Scientific Inc., USA). Further analytical details regarding calibration, reproducibility and autosampling method can be found in Osmont et al. (2018). The samples were subsequently analyzed for 13 ions (5 cations: ammonium NH_4^+, calcium Ca^{2+}, magnesium Mg^{2+}, potassium K^+ and sodium Na^+; and 8 anions: acetate CH_3COO^-, chloride Cl^-, fluoride F^-, formate $HCOO^-$, methanesulfonate (MSA) $CH_3SO_3^-$, nitrate NO_3^-, oxalate $C_2O_4^{2-}$ and sulfate SO_4^{2-}) by ion chromatography (850 Professional I*C*, Metrohm, Switzerland).

To estimate microscopic charcoal concentrations, we added a known amount of *Lycopodium* marker spores to the six snow samples dedicated to palynological analyses, and prepared the samples following the evaporation-based protocol for ice samples developed by Brugger et al. (2018b). Microscopic charcoal particles were identified as completely opaque particles with a major axis >10 µm and with angular shape following Tinner and Hu (2003). We counted to a combined sum of 200 items (microscopic charcoal + *Lycopodium* spores; Finsinger and Tinner, 2005).

2.4 Air mass trajectories and transport simulations

To link the observations in the snowpack with the fire emissions in Portugal, we calculated ~~three~~ 5-day backward trajectories at a 6-hourly resolution with the Lagrangian analysis tool LAGRANTO (Sprenger and Wernli, 2015) based on ERA-Interim reanalysis data (Dee et al., 2011). The trajectories started at the coordinates of JFJ, at 20 equidistant levels in pressure coordinates between 700 hPa and ~~200~~ 500 hPa, in accordance with the detected smoke plume height.

We used the global aerosol-climate model ECHAM6.3-HAM2.3 to simulate the transport of BC and microscopic charcoal (Gilgen et al., 2018; Stier et al., 2005; Zhang et al., 2012). To the best of our knowledge, this is the only model with a charcoal module implemented. The large-scale wind velocities of the simulations were nudged towards ERA-Interim reanalysis data. Two simulations were conducted: i) a simulation without any fire emissions and ii) a simulation including the fire emissions that occurred in Central Portugal (−8.45° to −7.85° E; 39.75° to 40.25° N) in June. Daily fire emission fluxes were calculated from the Fire Inventory from NCAR (FINN version 1.6.; Wiedinmyer et al., 2011) and interpolated to the model grid. For anthropogenic aerosol emissions, we used ACCMIP (Atmospheric Chemistry and Climate Model Intercomparison Project) interpolated emissions for the year 2008 (Lamarque et al., 2010), being constant over the year. A spatial resolution of T127L95 was applied (≈100 km at the equator). To simulate the microscopic charcoal particles, we chose a density of 0.6 g cm^{-3}, a geometric mean radius upon emission of 5 µm, a threshold radius of 4.9 µm and a scaling factor of BC mass emissions of 250. These parameters were extensively tested, compared and validated by Gilgen et al. (2018).

2.5 Satellite observations

To analyze the fire source itself, i.e. the spatial and temporal extent as well as the intensity of the burning near Pedrógão Grande, we used different fire products retrieved from satellite imagery over the study area. The fires were detected by several satellite sensors and during multiple overpasses (e.g. Visible Infrared Imaging Radiometer Suite (VIIRS), Moderate Resolution Imaging Spectroradiometer (MODIS) or Advanced Very High Resolution Radiometer (AVHRR)), which allows to study the temporal evolution (i.e. progression) of the fires. In consistency with FINN v1.6, we chose the Thermal Anomalies & Fire Daily L3 Global Product, which is also utilized for the emission model. In addition, we obtained the Burned Area Monthly L3 Global Product of MODIS~~Here, we chose the Thermal Anomalies & Fire Daily L3 Global Product, which is also utilized for the FINN emission model, together with the Burned Area Monthly L3 Global Product of MODIS~~.

The MODIS sensors on board NASA's Earth Observing System Terra and Aqua satellites have a return period of one to two days with a daytime equator crossing time at 10:30 am (1:30 pm) for Terra (Aqua). The areal extent of the study site was defined as −8.45° to −7.85° longitude and 39.75° to 40.25° latitude according to the location of the forest fires and also used for the modelling (see Section 2.4). For June 2017, we downloaded the respective tiles over the study area of both products: i) the 1 km daily thermal anomaly and fires MOD14A1 (MODIS/Terra) and MYD14A1 (MODIS/Aqua: both V006; Giglio et al., 2015a) products and ii) the monthly 500m Burned Area Product MCD64A1 (V006; Giglio et al., 2015b). The latter is a combined product of the burned area detected by the MODIS sensors onboard the Terra and Aqua satellites. It was resampled to a spatial resolution of 1 km. The tiles of the MOD14A1/MYD14A1 products were mosaicked into one image. We lastly reprojected the scenes of both products accordingly to the FINN emission data (version 1.6; Wiedinmyer et al., 2011). Both products were analyzed in terms of active fire progression, fire radiative power (FRP), burned area date and extent, and cloud coverage. Moreover, we compared them with the spatial distribution of emission species, like BC, NO_x and $PM_{2.5}$, derived from the FINN database.

To detect the fire plume, we analyzed different daily Aerosol Optical Depth (AOD) products from OMAEROe v003 at 0.25° (smallest spatial resolution in the GIOVANNI database), MODIS-Terra MOD08_D3 v6.1. at 1° spatial resolution, and from the Modis sensor flying onboard of the satellites Terra and Aqua at a spatial resolution of 10 km at nadir and their area-averaged time series for 17th until 26th of June.

3 Results and discussions

3.1 Snowpit profile

The snowpit profile (Fig. 2b) showed five layers with different grain size and density (Fig. 2c). Layer A, from 0 to 10 cm depth (d = 0.2 g cm^{-3}), was composed of fresh and very light powder snow corresponding to the snowfall on 29th June. Layer B, from 10 to 22 cm (d = 0.37, g cm^{-3}) was made of light snow probably originating from the snowfall on 28th June. Snow in layer C, from 22 to 50 cm (d = 0.54 g cm^{-3}), already experienced some transformation as bigger (2–3 mm) round-shaped grains were

observed that could relate to the snowfalls that occurred on 25th and 26th June. For those days, a good agreement was obtained between the precipitation amount from Itramen and the snow layer height corrected for density (Fig. 2a), confirming our time attribution. Below 50 cm depth, accurate dating becomes impossible, but the frequent presence of ice layers and more compact snow indicates melting due to warmer temperatures. This is in line with the June 2017 heat wave in Switzerland that lasted from 19th to 24th June (MétéoSuisse, 2017). Layer D, from 50 to 76 cm depth, was composed of denser and compact snow (d = 0.55 g cm^{-3}). Lastly, below 78 cm depth, layer E seemed even more compact, although the density did not significantly change (d = 0.52 g cm^{-3}).

3.2 Fire tracers: rBC, microscopic charcoal and major ions

A ~~remarkable~~ peak with concentrations up to 9.8 ng g^{-1} is visible in the rBC profile (Fig. 2d) from 22 to 37 cm depth (samples 4 to 6; layer C), corresponding to the first snowfalls recorded after the event. This suggests that atmospheric BC was probably scavenged by snow on 25th and 26th June, which is in agreement with a drop in atmospheric eBC concentration observed simultaneously (Fig. 2a). Wet deposition seems to be the preferential pathway as the rBC peak is spread over the whole accumulated snow layer while dry deposition would rather create a thin and highly concentrated layer. Several studies indicate that rBC is mainly scavenged from the atmosphere via wet deposition processes (Cape et al., 2012; Ruppel et al., 2017; Sinha et al., 2018). The uppermost two layers (A–B, samples 1 to 3) show very low rBC concentrations (average: 0.21 ng g^{-1}), in agreement with the clean atmospheric conditions that prevailed on 28th and 29th June with eBC concentrations below 10 ng m^{-3}. Below the rBC peak, a secondary rBC maximum with 4.5 ng g^{-1} was observed between 60 and 70 cm in one replicate series, but otherwise average concentrations are low ~~from 37 to 110 cm depth, rBC concentrations with an average of (~~2.0 ng g^{-1} ~~)show some variability but no clear trend or peak~~. Except for this secondary maximum, a~~A~~ very good agreement is obtained between the two series of replicate rBC samples (r = 0.90, all samples).

The microscopic charcoal record (Fig. 2e) shows a smaller peak at 60–70 cm depth (4000 fragments L^{-1}), and the main maximum at 30–40 cm depth, reaching a factor of 10 higher concentrations (20 000 fragments L^{-1}) compared to the average of all six samples. We relate the main peak to the fire event in Portugal. Compared to the rBC peak, the narrower microscopic charcoal peak could indicate ~~either~~ a more important contribution of dry deposition versus wet deposition ~~or a more efficient scavenging during snowfall~~, ~~possibly due~~ consistent with~~to~~ its larger particle size (> 10 µm major axis for microscopic charcoal vs. < 1 µm diameter for rBC). Microscopic charcoal is a specific proxy for biomass burning, whereas rBC is less specific and can also originate from fossil fuel combustion. ~~The simultaneous rBC and microscopic charcoal peaks (rBC samples 4 to 6 and microscopic charcoal sample 2, respectively) provide evidence for a common biomass burning source and transport within the plume.~~ No ice layer was observed in the uppermost 50 cm of the snowpit, which indicates that both rBC and microscopic charcoal profiles were not affected by melting processes.

The mass size distribution for the broadband low gain (BBLG) channel of the SP2 remained similar throughout the profile with 306 nm and 291 nm for the two series of replicates, respectively (Fig. 2d). This indicates that rBC size distributions in the falling snow are rather stable, as already observed by Sinha et al. (2018). Only sample 13 shows a bigger fraction of large

rBC particles, in association with a small peak in rBC and charcoal concentration.~~,~~ On the contrary, no shift in the rBC size distribution is visible for samples 4 to 6 during the peak in rBC and charcoal concentrations. ~~The rather large diameter of the rBC particles, with a mean mode of the rBC mass size distribution for the broadband high gain (BBHG) channel of the SP2 of 306 nm and 291 nm for the two series of replicates, respectively (Fig. 2d), also suggests a predominant biomass burning origin. This is in agreement with Lim et al. (2017), who observed a mean mass mode diameter of 290.8 nm in the summer layers of the Elbrus ice core and attributed the size increase compared to winter layers to the predominance of forest fires and/or agricultural fires as rBC source in summer. The mass size distribution remains fairly similar throughout the profile and does not display higher values in the samples containing rBC peak concentrations. This indicates that rBC size distributions in the falling snow are rather stable, as already observed by Sinha et al. (2018). Only sample 13 shows a bigger fraction of large rBC particles, in association with a small peak in rBC and charcoal concentration, potentially suggesting more local burning sources. On the contrary, no shift in the rBC size distribution is visible for samples 4 to 6 during the peak in rBC and charcoal concentrations.~~

Continental-scale calibrations comparing satellite-based fire incidence and charcoal influx into lake sediment or peat bogs suggest that microscopic charcoal particles > 10 µm mainly originate from regional sources with an average radius of ca. 40 km (Adolf et al., 2018). However, previous studies of charcoal in ice cores indicate that charcoal can be transported over distances larger than 500 km (e.g. Brugger et al., 2018a; Eichler et al., 2011; Reese et al., 2013, Hicks and Isaksson, 2006). These differences can be explained by dissimilar environmental conditions, as lake sediment and peat bog studies are usually performed at low-elevation sites surrounded by potential burning sources while snowpits and ice cores originate from high-latitude or high-altitude sites remote from vegetation (Brugger et al., 2018a, 2019b). These remote sites frequently lie within the free troposphere: for JFJ, free troposphere background conditions are observed about 39% of the time, with a maximum of 60% in winter and a minimum of 20% in summer (Bukowiecki et al., 2016). However, a travel distance from Portugal to JFJ of around 1500 km seems exceptional. Given the strong intensity of this fire (see Section 3.5), we hypothesize that convection lifted a large amount of microscopic charcoal particles high up in the atmosphere enabling the long-distance travel. The microscopic charcoal peak concentrations observed in this study are outstandingly high and only comparable to exceptional peak events in other ice cores (Brugger et al., 2018a; Eichler et al., 2011; Reese et al., 2013), which might be due partly to the highly resolved sampling. This is in contrast to rBC, for which such peak concentrations have been observed in the preindustrial part of European high-altitude ice cores, when rBC mainly originated from biomass burning (Lim et al., 2017; Sigl et al., 2018).

In addition to rBC and charcoal, ions such as ammonium (NH_4^+), formate ($HCOO^-$), acetate (CH_3COO^-) and nitrate (NO_3^-) have been used as fire tracers (Arienzo et al., 2017; Fischer et al., 2015; Legrand et al., 2016; Savarino and Legrand, 1998), although other emission sources exist, such as direct biogenic emissions (ammonium, formate), oxidation from volatile organic compounds (formate, acetate) and anthropogenic sources (agriculture for ammonium, traffic and agriculture for nitrate). Except for a few values, a good agreement was obtained between the two sets of replicates of the major ion profiles, particularly for

ammonium and nitrate (Fig. 3). None of the ionic fire tracers shows increased concentrations ~~Surprisingly, these ions do not display any significant enhancement of their concentration~~ at the depth of the rBC peak (~~from~~ 22~~ to~~ 37 cm).

We hypothesize that charcoal originating from the Portugal fires was deposited by dry deposition during the period 22nd to 24th June, when the fire plume arrived at the JFJ as detected by elevated atmospheric eBC concentrations. Since no snowfall occurred during that period, the majority of BC was not deposited. Dry deposition most likely resulted in a confined charcoal layer, which was not separated from the rBC peak in the snowpit due to the coarse sampling resolution of 10 cm. With the beginning of snowfall on 25th June, air mass transport changed, ending the advection of the fire plume to the JFJ as indicated by backward trajectories (see below and Fig. 4). Instead more regional, polluted air masses were scavenged, which explains the absence of ionic fire tracers and of a shift in the rBC size distribution. ~~depth, showing that, under present day conditions, even an exceptional fire event does not necessarily result in an exceptional peak of ammonium, formate, acetate or nitrate. This is mainly the result of the predominance of other emission sources (biogenic and anthropogenic emissions). To a lesser extent, varying atmospheric lifetimes compared to rBC and microscopic charcoal, and different sensitivities to wet deposition (different scavenging ratios) might also explain these differences. Among the ionic species, only calcium shows a concomitant peak with rBC and microscopic charcoal. One possible explanation is that snowfalls on 25th and 26th June were the first ones following the June 2017 heat wave in Switzerland. Dust concentrations might have been elevated during this dry and warm period and those subsequent snowfalls could have cleaned the atmosphere and led to wet deposition of dust-related ions such as calcium.~~

3.3 rBC scavenging ratios

rBC scavenging ratios (W) were calculated to determine the total scavenging of rBC from air to snow by snowfall, based on the following formula: $W = \rho C_s/C_a$, with ρ the air density in g m^{-3}, C_s the concentration of rBC in snow in ng g^{-1} and C_a the concentration of rBC in air in ng m^{-3} (Schwikowski et al., 1995). For C_a, we considered the daily average eBC concentration on 24th June, just before the precipitation starts, while for C_s, we used the average of samples 4–6 of the snowpit, corresponding to the days 25th and 26th June when peak values are found. The air density at JFJ of 842 g m^{-3} was calculated with the ideal gas law using a temperature of 273.15 K and a pressure of 66000 Pa obtained from MeteoSwiss for the JFJ weather station.

In our case, the calculation of rBC scavenging ratios (Table 1) is highly dependent on the choice of a mass absorption coefficient (MAC) for converting the light absorption intensity given by the MAAP into an eBC concentration. The objective is that the eBC mass concentrations from the MAAP precisely match the rBC mass concentrations from the SP2, in order not to introduce a methodological bias as two different quantification methods are used. Previous studies suggested a median MAC of 10.2 ± 3.2 m^2 g^{-1} for JFJ (Liu et al., 2010) or 11.1 ± 0.2 m^2 g^{-1} in summer (Cozic et al., 2008). Higher values (13.3 ± 3.0 m^2 g^{-1}) have also been reported in the case of eBC from a purely biomass burning origin (Schwarz et al., 2008). An upper limit estimate of 20 m^2 g^{-1} for the MAC was obtained during the CLACE 2016 summer campaign at JFJ (Motos et al., 2019). This value is of particular interest as both a MAAP and a SP2 were simultaneously sampling the air at JFJ during this campaign. By applying a MAC of 20 m^2 g^{-1}, a perfect agreement could be obtained between the BC mass concentrations given by the

MAAP and those given by SP2 (measurements not shown). Therefore, MACs of 10 and 20 m^2 g^{-1} were chosen here (λ = 637 nm) to test the lower and upper limits, leading to a range of scavenging ratios from 41 to 91 (Table 1).

Few BC air-to-snow scavenging ratio values are available in the literature, usually ranging from 100 to 150 (Table 2). By comparing our scavenging ratios obtained at JFJ with values from previous studies, it appears that the choice of a MAC value of 20 m^2 g^{-1} seems preferable. Discrepancies can arise from the different locations implying various climatic conditions, from the use of different methods to quantify BC (light absorption, thermal-optical or incandescence), and from the different relative contribution of wet and dry deposition processes, depending on the location and elevation, with higher scavenging ratios at higher altitudes (Gogoi et al., 2018).

3.4 Atmospheric transport

The ~~3~~5-day air mass backward trajectory analyses suggest Portugal as a very likely source for the atmospheric eBC (Fig. 4). For all the days between the 22nd and the 2~~4~~5th June, when atmospheric ~~as well as deposited~~ eBC concentrations were ~~large~~high, part of the air masses originated from Portugal, which is also supported by simulations from MeteoSwiss (MeteoSwiss, 2017). The back trajectories with arrival at JFJ on 25th June at 18 UTC indicate a major change in the synoptic situation to more north-westerly flow directions. We can only speculate that this happened concomitant with the onset of precipitation, since the timing of the latter is not precisely known. AOD data at 10 km resolution support that between 20th and 22nd of June the JFJ site received air masses with elevated AOD from Portugal. The AOD levels increased over Switzerland mainly north of the Alps during that time, in agreement with the backward trajectories (Fig. 4). From 23rd to 25th of June the area was cloud covered, so AOD could not be retrieved. Simulations with ECHAM-HAM show no clear difference for BC when we compare the simulation with fires to the simulation without fires (Fig. 5). In our simulations, BC is preferentially removed by wet scavenging. This suggests that the simulated BC deposition peak observed from 26th to 28th June is mainly reflecting the precipitation pattern~~, as precipitation frequently occurred at JFJ from June 25th on (Fig. 2a), and not a change in emission sources~~. Furthermore, other BC sources than fires seem to dominate in our simulations, which ~~.~~ is in agreement with our hypothesis that during fire plume arrival at JFJ the majority of fire-related BC was not deposited due to the lack of snowfall. With the beginning of snowfall at JFJ, air mass transport changed and more regional polluted air masses with minor or without fire contribution were scavenged. ~~This could be due to the~~In addition, the relatively low spatial resolution of the model~~, which~~ smooths the topography, ~~as well as due~~ resulting in a ~~to the~~more efficient vertical mixing in the lower troposphere ~~in the model~~. As a consequence, overestimated levels of BC from regional anthropogenic sources can probably reach the location of JFJ in the model compared to reality~~, and therefore mask the BC peak related to the Portuguese fires~~.

Microscopic charcoal has no other sources than biomass burning in our model. We observe a clear peak in the deposited microscopic charcoal fluxes on the 23rd ~~of~~ June (Fig. 5), which is predominantly caused by dry removal processes (i.e. dry deposition and gravitational settling) and near the observed peak on the 22nd ~~of~~ June for atmospheric eBC (Fig. 2a). The simulated deposition fluxes are still rather high on the 25th of June, suggesting that dry deposition continued for the entire fire episode at JFJ~~when the observed peak in microscopic charcoal starts (Fig. 2e)~~. An exact temporal match cannot be expected

due to the daily resolution of the fire emissions and the rather low spatial resolution of the model together with the dating uncertainties of the snow pit. Nevertheless, this result qualitatively confirms the hypothesis that the microscopic charcoal particles observed at JFJ originated from Portugal.

3.5 Observations by satellites

Quantification of the occurrence (active fires), intensity (maximum FRP) and extent (burned area) provided by satellite products allows the modelling of biomass burning emissions. Here, we analyzed the temporal and spatial extent as well as the FRP of the wildfires with the MODIS thermal anomaly and fire (MOD14A1/MYD14A1) and the MCD64A1 burned area products together with emission species of the FINN v1.6. database. The fires evolved on the 17th June 2017 in the afternoon (Fig. 6a) in a central location between the fire clusters. An additional comparison of the Aqua/MODIS and VIIRS/NPP Active Fire Product (375 m spatial resolution; Schroeder at el., 2014) showed, that the fire was early detected by the VIIRS/NPP Fire Product at ~13:46 UTC. The fire was located few kilometres away from a thick cumulonimbus cloud. Though, the overpass time of Aqua/MODIS was almost simultaneous (i.e. 13:45-13:50 UTC), the fire was too small to be detected by the coarser spatial resolution sensor (1 km). This explains why FINN v1.6 has no emission entries for 17th June. Later during the day, several fires were already burning according to the burned area product, which indicates a fast spread in south- and northward direction. Clouds obscured observation by the MODIS sensor on the 18th June. Therefore, fewer active fires and lower maximum FRP were detected on this day, resulting in gaps in the MOD14A1/MYD14A1 product (Fig. 6a). However, the MCD64A1 burned area product shows the day by day evolution of the fires, forming two big fires clusters. The maximum fire activity and vegetation consumption was observed on the 19th and 20th, as indicated by the burned area and the high maximum FRP values. Less powerful fires on the south and mainly north edges of the two fire clusters burned from the 20th to 22nd until the fires were completely extinguished on the 24th of June.

The total area burned over these days accumulates to 501 km^2 according to the burned area product. The total area might be underestimated by this product compared to the maximum FRP, which indicates a larger spatial extent of burning. The detection signals of the burned area were probably too low to detect the burned area along the outer edges of the fires in the south and north (Fig. 6a). Nevertheless, this area agrees well with the actual burned area of 470 km^2 for the two major fire outbreaks occurring in the municipalities of Pedrógão Grande and Góis, based on ground observations (CTI, 2017). The modelled BC emissions (Fig. 6b), based on the FINN v1.6. database, range from less than 500 kg day^{-1} $pixel^{-1}$ to over 2250 kg day^{-1} $pixel^{-1}$. A total of about 203.5 tons of BC was emitted by this exceptional fire event (Table 3). Due to cloud obscuration and masking on 18th June, this value is probably underestimated.

3.6 Deposition fluxes

Deposition fluxes were calculated for rBC and microscopic charcoal by multiplying the concentration of the respective compounds by the snow accumulation corrected for density. Even if these values remain uncertain due to dating limitations of the snowpit and to the lack of detailed snowfall monitoring at JFJ, preventing us from knowing the exact duration of a snowfall

event, they constitute the first step towards a quantitative transfer function~~. In the case of BC, mainly wet deposited, another difficulty is the high dependency on the time of the precipitation event. Here, the highest atmospheric concentrations on 22nd June were not archived since the precipitation event in the form of snow took place on 25th June, depositing only the remaining BC particles~~.

For microscopic charcoal, ~~in the case of June 25th (peak day), we obtained~~we observed a ~~daily~~ total deposition flux of 104 fragments cm^{-2}~~12 fragments m^{-2} s^{-1}, i.e. 37,800 fragments cm^{-2} yr^{-1}~~ in the snowpit, around ~~20~~ 8 times more than the modelled flux of 13.8 fragments cm^{-2} (integral over 23rd and 24th June, Fig. 5). Compared to yearly average fluxes from high-alpine ice archives (Table 4), the estimated influx at JFJ during the event is exceptional and cannot be explained by the somewhat lower altitude of the JFJ site compared to the other alpine ice-core locations. The comparison ~~with other ice archives~~ suggests this single outstanding event deposited nearly as many charcoal particles ~~per day (104 fragments cm^{-2} day^{-1})~~ as during an average year in other ice archives (e.g. Brugger et al. 2018a).

For rBC, the total deposition flux for samples 4, 5, and 6 was 62 ng cm^{-2} (average of replicate samples). The integral flux retrieved from the model for 26th, 27th, and 28th June is 195 ng cm^{-2} (Fig. 5); a factor of three higher than the observation. Interestingly, the model underestimates the charcoal and overestimates the BC flux. When the model performance was evaluated previously with longer-term charcoal deposition fluxes, the opposite was observed (Gilgen et al., 2018). It was hypothesized that the model overestimates the fluxes at ice core sites because of their high location within complex topography. The model is not able to simulate these high locations correctly, since the surface altitude is constant over the whole grid box; i.e. the topography is smoothed. In addition, ice core sites are often located above the top plume height of most fires (Rémy et al., 2017), which may prevent transport of charcoal particles to them. Obviously the Pedrógão Grande case was exceptional, since the plume was transported at elevations between 3000 and 5000 m a.s.l.. In addition, an underestimation of the fire emissions might have played a role for the charcoal flux. Contrary to the effect on charcoal, the smoothed topography in the model and the corresponding more efficient vertical mixing might have resulted in overestimated levels of BC from regional anthropogenic sources, explaining the overestimation of the BC flux. ~~considering both June 25th and 26th and a cumulative snowfall duration of only 6 hours per day, as rBC is mainly wet deposited and snowfalls were intermittent on those days as shown by the JFJ webcam, deposition fluxes amount to 1420 ng m^{-2} s^{-1}. These values are two orders of magnitude higher than the modelled deposition fluxes (Fig. 5), which could be due to an underestimation of the fire emissions or result from both modelled and experimental uncertainties. Such l~~Large discrepancies between modelled and actual deposited rBC fluxes were already pointed out by Thomas et al. (2017), who found a factor of 2–100 in a case study from Greenland and advocated for a better description of precipitation scavenging and fire emissions by the models.

Conclusions

In this case study, biomass burning emissions from an outstanding fire event in Portugal in June 2017 were observed at the high-alpine site Jungfraujoch, Swiss Alps, in both the atmosphere and the snowpack. According to satellite observations, the

fire burned a total area of 501 km^2 from 17th to 24th June, in close agreement with ground observations. At least about 203.5 tons of BC were emitted during this event. Atmospheric backward trajectory analyses showed that the resulting plume of smoke traveled three days before reaching Switzerland, leading to a peak in atmospheric eBC at JFJ on 22nd June, lasting until 25th June when snowfall occurred. ~~, therefore archiving rBC and microscopic charcoal in the snowpack.~~ Dry deposition of microscopic charcoal resulted in an outstanding peak in the snowpack. ~~Outstanding concentrations and~~ This event deposited nearly as many charcoal particles as during an average year in other ice archives~~influx were observed for microscopic charcoal~~. Our study highlights that, for microscopic charcoal, snow and ice archives are more sensitive to distant ~~events~~ fires than sedimentary archives, due to the special settings at high elevation. For snow and ice archives, it also reveals that a much longer traveling distance (≈1500 km) than previously thought can be reached, with outstandingly high concentrations in the case of events with optimal ~~climate~~ weather and transport conditions, thus making microscopic charcoal an excellent biomass burning tracer in ice archives. For rBC, in contrast, concentrations in the snow were not exceptionally high. In combination with the absence of a peak in ionic fire tracers such as ammonium, this suggest that ~~On the contrary,~~ the majority of atmospheric BC was not deposited during the fire episode due to a lack of precipitation. Instead the observed rBC peak was mostly likely caused by scavenging of air masses containing regional pollution with the beginning of snowfall on 25th June, which ended the advection of the fire plume to the JFJ~~rBC concentrations were not exceptionally high~~. rBC scavenging ratios were in line with previous studies, giving additional evidence that rBC ~~seemed to be~~was predominantly scavenged by wet deposition~~, with scavenging ratios of 81–91, in line with previous studies~~. Simulations with a global aerosol climate model supported that the observed microscopic charcoal particles ~~probably~~ originated from the fires in Portugal, whereas their contribution to the BC signal in snow was minor. ~~For BC, the model did not reproduce the observed signal due to the predominance of other emission sources, while for charcoal, a better agreement was observed as charcoal does not have other emission sources than fires.~~ The findings of our~~Such~~ case study~~ies~~ are important for future ice-core studies, as they document that for BC as fire tracer the signal preservation depends on precipitation and wet deposition. Single events, like this example, might not be preserved due to unfavorable meteorological conditions. ~~how biomass burning information is preserved in snow archives.~~ Nevertheless, an exhaustive quantification of the process remains challenging due to the intrinsic uncertainties of each parameter, which requires further collaboration between the different disciplines involved.

Author contributions

DO designed the project, carried out sampling, performed rBC analyses and wrote the paper. SB performed microscopic charcoal analyses and contributed to the manuscript writing. AG made atmospheric transport simulations and contributed to the manuscript writing. HW retrieved and analyzed satellite data and contributed to the manuscript writing. MiS organized and led the snowpit study, and commented the manuscript. RLM provided the eBC data from JFJ and advice to interpret them, and commented the manuscript. CS, WT and SW contributed to the manuscript writing. MaS led the project, ~~commented~~ contributed to and supervised writing of the manuscript.

Competing interests

The authors declare that they have no conflict of interest.

Acknowledgements

We thank the Swiss National Science Foundation (SNF) for granting the Sinergia project "Paleo fires from high-alpine ice cores", which funded this research (CRSII2_154450). Furthermore, we thank Nicolas Bukowiecki for providing the atmospheric eBC data from Jungfraujoch, the Institute for Snow and Avalanche Research (SLF) for the precipitation data and Sabina Brütsch for ion chromatography analyses. The online eBC measurements at Jungfraujoch were conducted with financial support from MeteoSwiss (GAW-CH aerosol monitoring program) and from the European Union as well as the Swiss State Secretariat for Education, Research and Innovation (SERI) for the European Research Infrastructure for the observation of Aerosol, Clouds and Trace Gases (ACTRIS). The International Foundation High Altitude Research Station Jungfraujoch and Gornergrat (HSFJG) is acknowledged for hosting the online aerosol measurements and for giving access for snow sampling. The authors gratefully acknowledge the personal communication and data provided by C. Wiedinmyer, Cooperative Institute for Research and Environmental Sciences (CIRES), University of Colorado Boulder, Boulder, USA. The modelling was supported by a grant from the Swiss National Supercomputing Centre (CSCS) under project ID s652. The ECHAM-HAMMOZ model is developed by a consortium composed of ETH Zürich, Max Planck Institut für Meteorologie, Forschungszentrum Jülich, the University of Oxford, the Finnish Meteorological Institute, and the Leibniz Institute for Tropospheric Research, and managed by the Center for Climate Systems Modeling (C2SM) at ETH Zürich. The MOD14A1/MYD14A1 and MCD64A1 data products were retrieved from the online Data Pool, courtesy of the NASA Land Processes Distributed Active Archive Center (LP DAAC), USGS/Earth Resources Observation and Science (EROS) Center, Sioux Falls, South Dakota, https://lpdaac.usgs.gov/data_access/data_pool.

References

Adolf, C., Wunderle, S., Colombaroli, D., Weber, H., Gobet, E., Heiri, O., van Leeuwen, J. F. N., Bigler, C., Connor, S. E., Gałka, M., La Mantia, T., Makhortykh, S., Svitavská-Svobodová, H., Vannière, B., and Tinner, W.: The sedimentary and remote-sensing reflection of biomass burning in Europe, Global Ecol. Biogeogr., 27, 199–212, 2018.

Andreae, M. O. and Merlet, P.: Emission of trace gases and aerosols from biomass burning, Global Biogeochem. Cy., 15(4), 955–966, 2001.

Arienzo, M. M., McConnell, J. R., Murphy, L. N., Chellman, N., Das, S., Kipfstuhl, S., and Mulvaney, R.: Holocene black carbon in Antarctica paralleled Southern Hemisphere climate, J. Geophys. Res.-Atmos., 122, 2017.

Baltensperger, U., Gäggeler, H. W., Jost, D. T., Lugauer, M., Schwikowski, M., and Weingartner, E.: Aerosol climatology at the high-alpine site Jungfraujoch, Switzerland, J. Geophys. Res., 102(D16), 19707–19715, 1997.

Bond, W. J., Woodward, F. I., and Midgley, G. F.: The global distribution of ecosystems in a world without fire, New phytol., 165(2), 525–537, 2005.

Bowman, D. M. J. S., Balch, J. K., Artaxo, P., Bond, W. J., Carlson, J. M., Cochrane, M. A., D'Antonio, C. M., DeFries, R. S., Doyle, J. C., Harrison, S. P., Johnston, F. H., Keeley, J. E., Krawchuk, M. A., Kull, C. A., Marston, J. B., Moritz, M. A., Prentice, I. C., Roos, C. I., Scott, A. C., Swetnam , T. W., van der Werf, G. R., and Pyne, S. J.: Fire in the Earth System, Science, 324(5926), 481–484, 2009.

Bowman, D. M. J. S., Balch, J. K., Artaxo, P., Bond, W. J., Cochrane, M. A., D'Antonio, C. M., DeFries, R. S., Johnston, F. H., Keeley, J. E., Krawchuk, M. A., Kull, C. A., Mack, M., Moritz, M. A., Pyne, S. J., Roos, C. I., Scott, A. C., Sodhi, N. S., and Swetnam, T. W.: The human dimension of fire regimes on Earth, J. Biogeogr., 38(12), 2223–2236, 2011.

Brugger, S. O., Gobet, E., Sigl, M., Osmont, D., Papina, T., Rudaya, N., Schwikowski, M., and Tinner, W.: Ice records provide new insights into climatic vulnerability of Central Asian forest and steppe communities, Global Planet. Change, 169, 188–201, 2018a.

Brugger, S. O., Gobet, E., Schanz, F. R., Heiri, O., Schwörer, C., Sigl, M., Schwikowski, M., and Tinner, W.: A quantitative comparison of microfossil extraction methods from ice cores, J. Glaciol., 64(245), 432–442, 2018b.

Brugger, S. O., Gobet, E., Osmont, D., Behling, H., Fontana, S. L., Hooghiemstra, H., Morales-Molino, C., Sigl, M., Schwikowski, M., and Tinner, W.: Tropical Andean glacier reveals colonial legacy in modern mountain ecosystems, Quat. Sci. Rev., 2019a.

Brugger, S.O., Gobet, E., Blunier, T., Morales-Molino, C., Lotter, A. F., Fischer, H., Schwikowski, M., and Tinner, W.: Palynological insights into global change impacts on Arctic vegetation, fire, and pollution recorded in Central Greenland ice, Holocene, 29(7), 1189–1197, 2019b.

Bukowiecki, N., Weingartner, E., Gysel, M., Collaud Coen, M., Zieger, P., Herrmann, E., Steinbacher, M., Gäggeler, H. W., and Baltensperger, U.: A review of more than 20 years of aerosol observation at the high altitude research station Jungfraujoch, Switzerland (3580 m asl), Aerosol Air Qual. Res, 16, 764–788, 2016.

Cape, J. N., Coyle, M., and Dumitrean, P.: The atmospheric lifetime of black carbon, Atmos. Environ., 59, 256–263, 2012.

Clarke, A. D. and Noone, K. J.: Soot in the Arctic snowpack: a cause for perturbations in radiative transfer, Atmos. Environ., 19(12), 2045–2053, 1985.

Cozic, J., Verheggen, B., Weingartner, E., Crosier, J., Bower, K. N., Flynn, M., Coe, H., Henning, S., Steinbacher, M., Henne, S., Collaud Coen, M., Petzold, A., and Baltensperger, U.: Chemical composition of free tropospheric aerosol for PM1 and coarse mode at the high alpine site Jungfraujoch, Atmos. Chem. Phys., 8, 407–423, 2008.

CTI – Comissão Técnica Independente, Análise e apuramento dos factos relativos aos incêndios que ocorreram em Pedrógão Grande, Castanheira de Pera, Ansião, Alvaiázere, Figueiró dos Vinhos, Arganil, Góis, Penela, Pampilhosa da Serra, Oleiros e Sertã, entre 17 e 24 de junho de 2017, *Relatório*, Assembleia da República, 296 p., 2017.

Dee, D. P., Uppala, S. M., Simmons, A. J., Berrisford, P., Poli, P., Kobayashi, S., Andrae, U., Balmaseda, M. A., Balsamo, G., Bauer, P., Bechtold, P., Beljaars, A. C., van de Berg, L., Bidlot, J., Bormann, N., Delsol, C., Dragani, R., Fuentes, M., Geer,

A. J., Haimberger, L., Healy, S. B., Hersbach, H., Hólm, E. V., Isaksen, L., Kållberg, P., Köhler, M., Matricardi, M., McNally, A. P., Monge-Sanz, B. M., Morcrette, J., Park, B., Peubey, C., de Rosnay, P., Tavolato, C., Thépaut, J., and Vitart, F.: The ERA-Interim reanalysis: configuration and performance of the data assimilation system, Q.J.R. Meteorol. Soc., 137, 553–597, 2011.

Dibb, J. E., Talbot, R. W., Whitlow, S. I., Shipham, M. C., Winterle, J., McConnell, J., and Bales, R.: Biomass burning signatures in the atmosphere and snow at Summit, Greenland: An event on 5 August 1994, Atmos. Environ., 30(4), 553–561, 1996.

Eichler, A., Tinner, W., Brütsch, S., Olivier, S., Papina, T., and Schwikowski, M.: An ice-core based history of Siberian forest fires since AD 1250, Quaternary Sci. Rev., 30, 1027–1034, 2011.

Finsinger, W. and Tinner, W.: Minimum count sums for charcoal concentration estimates in pollen slides: accuracy and potential errors, Holocene, 15(2), 293–297, 2005.

Fischer, H., Schüpbach, S., Gfeller, G., Bigler, M., Rothlisberger, R., Erhardt, T., Stocker, T. F., Mulvaney, R., and Wolff, E.: Millennial changes in North American wildfire and soil activity over the last glacial cycle, Nat. Geosci., 8, 723–728, 2015.

Flannigan, M., Cantin, A. S., de Groot, W. J., Wotton, M., Nwebery, A., and Gowman, L. M.: Global wildland fire season severity in the 21st century, Forest Ecol. Manag., 294, 54–61, 2013.

Giglio, L., and Justice, C.: MOD14A1 MODIS/Terra Thermal Anomalies/Fire Daily L3 Global 1km SIN Grid V006 [Data set], NASA EOSDIS LP DAAC, doi: 10.5067/MODIS/MOD14A1.006, 2015a.

Giglio, L., Justice, C., Boschetti, L., and Roy, D.: MCD64A1 MODIS/Terra+Aqua Burned Area Monthly L3 Global 500m SIN Grid V006 [Data set], NASA EOSDIS Land Processes DAAC, doi: 10.5067/MODIS/MCD64A1.006, 2015b.

Gilgen, A., Adolf, C., Brugger, S. O., Ickes, L., Schwikowski, M., van Leeuwen, J. F. N., Tinner, W., and Lohmann, U.: Implementing microscopic charcoal particles into a global aerosol-climate model, Atmos. Chem. Phys., 18, 11813–11829, 2018.

Gogoi, M. M., Babu, S. S., Moorthy, K. K., Thakur, R. C., Chaubey, J. P., and Nair, V. S.: Aerosol black carbon over Svalbard regions of Arctic, Polar Sci., 10, 60–70, 2016.

Gogoi, M. M., Babu, S. S., Pandey, S. K., Nair, V. S., Vaishya, A., Girach, I. A., and Koushik, N.: Scavenging ratio of black carbon in the Arctic and the Antarctic, Polar Sci., 16, 10–22, 2018.

Gómez-González, S., Ojeda, F., and Fernandes, P. M.: Portugal and Chile: Longing for sustainable forestry while rising from the ashes, Environ. Sci. Policy, 81, 104–107, 2018.

Hantson, S., Pueyo, S., and Chuvieco, E.: Global fire size distribution is driven by human impact and climate, Global Ecol. Biogeogr., 24, 77–86, 2015.

Herren, P.-A., Eichler, A., Machguth, H., Papina, T., Tobler, L., Zapf, A., and Schwikowski, M.: The onset of Neoglaciation 6000 years ago in western Mongolia revealed by an ice core from the Tsambagarav mountain range, Quaternary Sci. Rev., 69, 59–69, 2013.

Hicks, S. and Isaksson, E.: Assessing source areas of pollutants from studies of fly ash, charcoal and pollen from Svalbard snow and ice, J. Geophys. Res., 111, D02113, 2006.

Jacobson, J.Z.: Climate response of fossil fuel and biofuel soot, accounting for soot's feedback to snow and sea ice albedo and emissivity, J. Geophys. Res., 109, D21201, 2004.

Jenk, T. M., Szidat, S., Schwikowski, M., Gaggeler, H. W., Brütsch, S., Wacker, L., Synal, H. A., and Saurer, M.: Radiocarbon analysis in an Alpine ice core: record of anthropogenic and biogenic contributions to carbonaceous aerosols in the past (1650-1940), Atmos. Chem. Phys., 6, 5381–5390, 2006.

Kaspari, S., Skiles, S. M., Delaney, I., Dixon, D., and Painter, T. H.: Accelerated glacier melt on Snow Dome, Mount Olympus, Washington, USA, due to deposition of black carbon and mineral dust from wildfire, J. Geophys. Res.-Atmos., 120(7), 2793–2807, 2015.

Keegan, K. M., Albert, M. R., McConnell, J. R., and Baker, I.: Climate change and forest fires synergistically drive widespread melt events of the Greenland Ice Sheet, P. Natl. Acad. Sci. USA, 111, 7964–7967, 2014.

Keywood, M., Kanakidou, M., Stohl, A., Dentener, F., Grassi, G., Meyer, C. P., Torseth, K., Edwards, D., Thompson, A. M., Lohmann, U., and Burrows, J.: Fire in the air: Biomass burning impacts in a changing climate, Crit. Rev. Env. Sci. Tech., 43(1), 40–83, 2013.

Konrad, H., Bohleber, P., Wagenbach, D., Vincent, C., and Eisen, O.: Determining the age distribution of Colle Gnifetti, Monte Rosa, Swiss Alps, by combining ice cores, ground-penetrating radar and a simple flow model, J. Glaciol., 59(213), 179–189, 2013.

Lamarque, J.-F., Bond, T. C., Eyring, V., Granier, C., Heil, A., Klimont, Z., Lee, D., Liousse, C., Mieville, A., Owen, B., Schultz, M. G., Shindell, D., Smith, S. J., Stehfest, E., Van Aardenne, J., Cooper, O. R., Kainuma, M., Mahowald, N., McConnell, J. R., Naik, V., Riahi, K., and van Vuuren, D. P.: Historical (1850–2000) gridded anthropogenic and biomass burning emissions of reactive gases and aerosols: methodology and application, Atmos. Chem. Phys., 10, 7017–7039, 2010.

Legrand, M., McConnell, J., Fischer, H., Wolff, E. W., Preunkert, S., Arienzo, M., Chellman, N., Leuenberger, D., Maselli, O., Place, P., Sigl, M., Schüpbach, S., and Flannigan, M.: Boreal fire records in Northern Hemisphere ice cores: a review, Clim. Past, 12, 2033–2059, 2016.

Legrand, M., and DeAngelis, M.: Light carboxylic acids in Greenland ice: A record of past forest fires and vegetation emissions from the boreal zone, J. Geophys. Res.-Atmos, 101(D2), 4129-4145, 1996.

Legrand, M., De Angelis, M.,Staffelbach, T., Neftel, A., and Stauffer, B.: Large perturbations of ammonium and organic acids content in the Summit-Greenland ice core: Fingerprint from forest fires?, Geophys. Res. Lett., 19(5), 473– 475, 1992.

Lim, S., Faïn, X., Ginot, P., Mikhalenko, V., Kutuzov, S., Paris, J.-D., Kozachek, A., and Laj, P.: Black carbon variability since preindustrial times in the eastern part of Europe reconstructed from Mt. Elbrus, Caucasus, ice cores, Atmos. Chem. Phys., 17, 3489–3505, 2017.

Liu, D., Flynn, M., Gysel, M., Targino, A., Crawford, I., Bower, K., Choularton, T., Jurányi, Z., Steinbacher, M., Hueglin, C., Curtius, J., Kampus, M., Petzold, A., Weingartner, E., Baltensperger, U., and Coe, H.: Single Particle Characterization of Black Carbon Aerosols at a Tropospheric Alpine Site in Switzerland, Atmos. Chem. Phys., 10, 7389–7407, 2010.

Marlon, J. R., Kelly, R., Daniau, A.-L., Vannière, B., Power, M. J., Bartlein, P., Higuera, P., Blarquez, O., Brewer, S., Brücher, T., Feurdean, A., Romera, G. G., Iglesias, V., Maezumi, S. Y., Magi, B., Courtney Mustaphi, C. J., and Zhihai, T.: Reconstructions of biomass burning from sediment–charcoal records to improve data–model comparisons, Biogeosciences, 13, 3225–3244, 2016.

MétéoSuisse, Bulletin Climatologique Juin 2017, Genève, 2017. Available at: https://www.meteosuisse.admin.ch/home/service-et-publications/publications.subpage.html/fr/data/publications/2017/7/bulletin-climatologique-juin-2017.html?pageIndex=5&tab=search_tab, last accessed 25.04.2019.

MeteoSwiss, Cendres des incendies portugais détectées en Suisse, https://www.meteosuisse.admin.ch/home.subpage.html/fr/data/blogs/2017/6/incendies-du-portugal-mesures-en-suisse.html, 2017, last accessed 08.10.2018.

Moritz, M. A., Batllori, E., Bradstock, R. A., Malcolm Gill, A., Handmer, J., Hessburg, P. F., Leonard, J., McCaffrey, S., Odion, D. C., Schoennagel, T., and Syphard, A. D.: Learning to coexist with wildfire, Nature, 515, 58–66, 2014.

Motos, G., Schmale, J., Corbin, J. C., Modini, R. L., Karlen, N., Bertò, M., Baltensperger, U., and Gysel-Beer, M.: Cloud droplet activation properties and scavenged fraction of black carbon in liquid-phase clouds at the high-alpine research station Jungfraujoch (3580m a.s.l.), Atmos. Chem. Phys., 19, 3833–3855, 2019.

Mouillot, F. and Field, C.: Fire history and the global carbon budget: a 1° × 1° fire history reconstruction for the 20th century, Global Change Biol., 11, 398–420, 2005.

Noone, K. J. and Clarke, A. D.: Soot scavenging measurements in Arctic snowfall, Atmos. Environ., 22(12), 2773–2778, 1988.

Osmont, D., Wendl, I. A., Schmidely, L., Sigl, M., Vega, C. P., Isaksson, E., and Schwikowski, M.: An 800-year high-resolution black carbon ice core record from Lomonosovfonna, Svalbard, Atmos. Chem. Phys., 18, 12777–12795, 2018.

Osmont, D., Sigl, M., Eichler, A., Jenk, T., and Schwikowski, M.: A Holocene black carbon ice-core record of biomass burning in the Amazon Basin from Illimani, Bolivia, Clim. Past, 15, 579–592, 2019.

Page, S. E., Siegert, F., Rieley, J. O., Boehm, H.-D. V., Jaya, A., and Limin, S.: The amount of carbon released from peat and forest fires in Indonesia during 1997, Nature, 420, 61–65, 2002.

Pechony, O. and Shindell, D. T.: Driving forces of global wildfires over the past millennium and the forthcoming century, P. Natl. Acad. Sci. USA, 107(45), 19167–19170, 2010.

Petzold, A. and Schönlinner, M.: Multi-angle absorption photometry – a new method for the measurement of aerosol light absorption and atmospheric black carbon, J. Aerosol Sci., 35, 421–441, 2004.

Petzold, A., Ogren, J. A., Fiebig, M., Laj, P., Li, S. M., Baltensperger, U., Holzer-Popp, T., Kinne, S., Pappalardo, G., Sugimoto, N., Wehrli, C., Wiedensohler, A., and Zhang, X. Y.: Recommendations for reporting "black carbon" measurements, Atmos. Chem. Phys., 13, 8365–8379, 2013.

Randerson, J. T., Liu, H., Flanner, M. G., Chambers, S. D., Jin, Y., Hess, P. G., Pfister, G., Mack, M. C., Treseder, K. K., Welp, L. R., Chapin, F. S., Harden, J. W., Goulden, M. L., Lyons, E., Neff, J. C., Schuur, E. A. G., and Zender, C. S.: The impact of boreal forest fire on climate warming, Science, 314, 1130–1132, 2006.

Reese, C. A., Liu, K. B., and Thompson, L. G.: An ice-core pollen record showing vegetation response to Late-glacial and Holocene climate changes at Nevado Sajama, Bolivia, Ann. Glaciol., 54(63), 183–190, 2013.

Rémy, S., Veira, A., Paugam, R., Sofiev, M., Kaiser, J.W., Marenco, F., Burton, S. P., Benedetti, A., Engelen, R. J., Ferrare, R., and Hair, J. W.: Two global data sets of daily fire emission injection heights since 2003, Atmos. Chem. Phys., 17, 2921–2942, 2017.

Ruppel, M. M., Soares, J., Gallet, J.-C., Isaksson, E., Martma, T., Svensson, J., Kohler, J., Pedersen, C. A., Manninen, S., Korhola, A., and Ström, J.: Do contemporary (1980–2015) emissions determine the elemental carbon deposition trend at Holtedahlfonna glacier, Svalbard?, Atmos. Chem. Phys., 17, 12779–12795, 2017.

Savarino, J. and Legrand, M.: High northern latitude forest fires and vegetation emissions over the last millennium inferred from the chemistry of a central Greenland ice core, J. Geophys. Res.-Atmos., 103(D7), 8267–8279, 1998.

Schwarz, J. P., Gao, R. S., Fahey, D. W., Thomson, D. S., Watts, L. A., Wilson, J. C., Reeves, J. M., Darbeheshti, M., Baumgardner, D. G., Kok, G. L., Chung, S. H., Schulz, M., Hendricks, J., Lauer, A., Karcher, B., Slowik, J. G., Rosenlof, K. H., Thompson, T. L., Langford, A. O., Loewenstein, M., and Aikin, K. C.: Single-particle measurements of midlatitude black carbon and light-scattering aerosols from the boundary layer to the lower stratosphere, J. Geophys. Res., 111, D16207, 2006.

Schroeder, W., Oliva, P., Giglio, L., and Csiszar, I. A.: The New VIIRS 375 m active fire detection data product: algorithm description and initial assessment. Remote Sens. Environ. 143, 85-96. doi: 10.1016/j.rse.2013.12.008, 2014.

Schwarz, J. P., Gao, R. S., Spackman, J. R., Watts, L. A., Thomson, D. S., Fahey, D. W., Ryerson, T. B., Peischl, J., Holloway, J. S., Trainer, M., Frost, G. J., Baynard, T., Lack, D. A., de Gouw, J. A., Warneke, C., and Del Negro, L. A.: Measurement of the mixing state, mass, and optical size of individual black carbon particles in urban and biomass burning emissions, Geophys. Res. Lett., 35, L13810, 2008.

Schwikowski, M., Seibert, P., Baltensperger, U., and Gäggeler, H. W.: A study of an outstanding Saharan dust event at the high-alpine site Jungfraujoch, Switzerland, Atmos. Environ., 29(15), 1829–1842, 1995.

Sigl, M., Abram, N. J., Gabrieli, J., Jenk, T. M., Osmont, D., and Schwikowski, M.: 19th century glacier retreat in the Alps preceded the emergence of industrial black carbon deposition on high-alpine glaciers, Cryosphere, 12, 3311-3331, 2018.

Sinha, P. R., Kondo, Y., Goto-Azuma, K., Tsukagawa, Y., Fukuda, K., Koike, M., Ohata, S., Moteki, N., Mori, T., Oshima, N., Førland, E. J., Irwin, M., Gallet, J.-C., and Pedersen, C. A.: Seasonal Progression of the Deposition of Black Carbon by Snowfall at Ny-Ålesund, Spitsbergen, J. Geophys. Res.-Atmos., 123, 997–1016, 2018.

Sprenger, M. and Wernli, H.: The LAGRANTO Lagrangian analysis tool – version 2.0, Geosci. Model Dev., 8, 2569–2586, 2015.

Stephens, M., Turner, N., and Sandberg, J.: Particle identification by laser-induced incandescence in a solid-state laser cavity, Appl. Optics, 42, 3726–3736, 2003.

Stier, P., Feichter, J., Kinne, S., Kloster, S., Vignati, E., Wilson, J., Ganzeveld, L., Tegen, I., Werner, M., Balkanski, Y., Schulz, M., Boucher, O., Minikin, A., and Petzold, A.: The aerosol-climate model ECHAM5-HAM, Atmos. Chem. Phys., 5, 1125–1156, 2005.

Thomas, J. L., Polashenski, C. M., Soja, A. J., Marelle, L., Casey, K. A., Choi, H. D., Raut, J.-C., Wiedinmyer, C., Emmons, L. K., Fast, J. D., Pelon, J., Law, K. S., Flanner, M. G., and Dibb, J. E..: Quantifying black carbon deposition over the Greenland ice sheet from forest fires in Canada, Geophys. Res. Lett., 44, 7965–7974, 2017.

Tinner, W. and Hu, F. S.: Size parameters, size-class distribution and area-number relationship of microscopic charcoal: relevance for fire reconstruction, Holocene, 13(4), 499–505, 2003.

Uglietti, C., Zapf, A., Jenk, T. M., Sigl, M., Szidat, S., Salazar, G., and Schwikowski, M.: Radiocarbon dating of glacier ice: overview, optimisation, validation and potential, Cryosphere, 10, 3091–3105, 2016.

Wang, Z. W., Gallet, J. C., Pedersen, C. A., Zhang, X. S., Ström, J., and Ci, Z. J.: Elemental carbon in snow at Changbai mountain, northeastern China: concentrations, scavenging ratios, and dry deposition velocities, Atmos. Chem. Phys., 14, 629–640, 2014.

Warren, S. G. and Clarke, A. D.: Soot in the atmosphere and snow surface of Antarctica, J. Geophys. Res., 95(D2), 1811–1816, 1990.

Weber and Wunderle, Drifting Effects of NOAA Satellites on Long-Term Active Fire Records of Europe, Remote Sens., 11(4), 467, 2019.

Wendl, I. A., Menking, J. A., Färber, R., Gysel, M., Kaspari, S. D., Laborde, M. J. G., and Schwikowski, M.: Optimized method for black carbon analysis in ice and snow using the Single Particle Soot Photometer, Atmos. Meas. Tech., 7, 2667–2681, 2014.

Wiedinmyer, C., Akagi, S. K., Yokelson, R. J., Emmons, L. K., Al-Saadi, J. A., Orlando, J. J., and Soja, A. J.: The Fire Inventory from NCAR (FINN): A High Resolution Global Model to Estimate the Emissions from Open Burning, Geosci. Model Dev., 4, 625–641, 2011.

Whitlow, S., Mayewski, P., Dibb, J., Holdsworth, G., and Twickler, M.: An ice-core-based record of biomass burning in the Arctic and sub-Arctic, 1750-1980, Tellus Series B-Chemical and Physical Meteorology, 46(3), 234-242, 1994.

Yalcin, K., Wake, C. R., Kreutz, K. J., and Whitlow, S. I.: A 1000-yr record of forest fire activity from Eclipse Icefield, Yukon, Canada, Holocene, 16(2), 200–209, 2006.

Zennaro, P., Kehrwald, N., McConnell, J. R., Schüpbach, S., Maselli, O. J., Marlon, J., Vallelonga,P., Leuenberger, D., Zangrando, R., Spolaor, A., Borrotti, M., Barbaro, E., Gambaro, A., and Barbante, C.: Fire in ice: two millennia of boreal forest fire history from the Greenland NEEM ice core, Clim. Past, 10, 1905–1924, 2014.

Zhang, K., O'Donnell, D., Kazil, J., Stier, P., Kinne, S., Lohmann, U., Ferrachat, S., Croft, B., Quaas, J., Wan, H., Rast, S., and Feichter, J.: The global aerosol-climate model ECHAM-HAM, version 2: sensitivity to improvements in process representations, Atmos. Chem. Phys., 12, 8911–8949, 2012.

Zhou, J., Tie, X., Xu, B., Zhao, S., Wang, M., Li, G., Zhang, T., Zhao, Z., Liu, S., Yang, S., Chang, L., and Cao, J.: Black carbon (BC) in a northern Tibetan mountain: effect of Kuwait fires on glaciers, Atmos. Chem. Phys., 18, 13673–13685, 2018.

Table 1: Values used for the calculation of rBC scavenging ratios (W) at Jungfraujoch, Switzerland. For air concentration (C_a), the eBC average value of June 24th was used, under two different MACs. For snow concentration (C_s), concentrations from the two sets of replicates were used.

MAC (m^2 g^{-1})	C_a (ng m^{-3})	C_s (ng g^{-1})	W
10	147.5	7.14–8.01	41–46
20	73.8	7.14–8.01	81–91

655

Table 2: Examples of BC scavenging ratios available in the literature.

Location	W	BC measurement quantity	Authors
Jungfraujoch (JFJ)	81–91	rBC/eBC	This study
Arctic	160	eBC	Clarke and Noone, 1985
Abisko, Sweden	97 ± 34	eBC	Noone and Clarke, 1988
Antarctica	150	eBC	Warren and Clarke, 1990
N-E China	140 ± 100	EC	Wang et al., 2014
Svalbard	98 ± 46	eBC	Gogoi et al., 2016
Antarctic	120 ± 23	eBC	Gogoi et al., 2018
Global	125	Modelled	Jacobson, 2004

Table 3: Burned area and BC emissions per day for the June 2017 forest fire in Portugal (*cloud covered).

Day	Burned area (km^2)	BC emissions (tons)
17th June	13	-
18th June	148*	53.7
19th June	243	99.8
20th June	45	25.5
21st June	30	24.5
22nd June	19	-
23rd June	3	-
Total	501	203.5

660

Table 4: Comparison of ~~yearly~~ microscopic charcoal influx at Jungfraujoch with the yearly average influx at selected glacier sites based on identical laboratory preparation and analytical methods.

Site	Altitude (m asl)	Microscopic charcoal influx (fragments cm^{-2} $year^{-1}$)	Reference
Jungfraujoch	3560	~~37800~~104*	This study
Tsambagarav (Mongolian Altai)	4100	200	Brugger et al. (2018a)
Colle Gnifetti (Swiss Alps)	4500	390	Gilgen et al. (2018)
Summit (Central Greenland)	3200	9	Brugger et al. (2019b)
Illimani (Bolivian Andes)	6300	130	Brugger et al. (2019a)

*This event only in fragments cm^{-2}

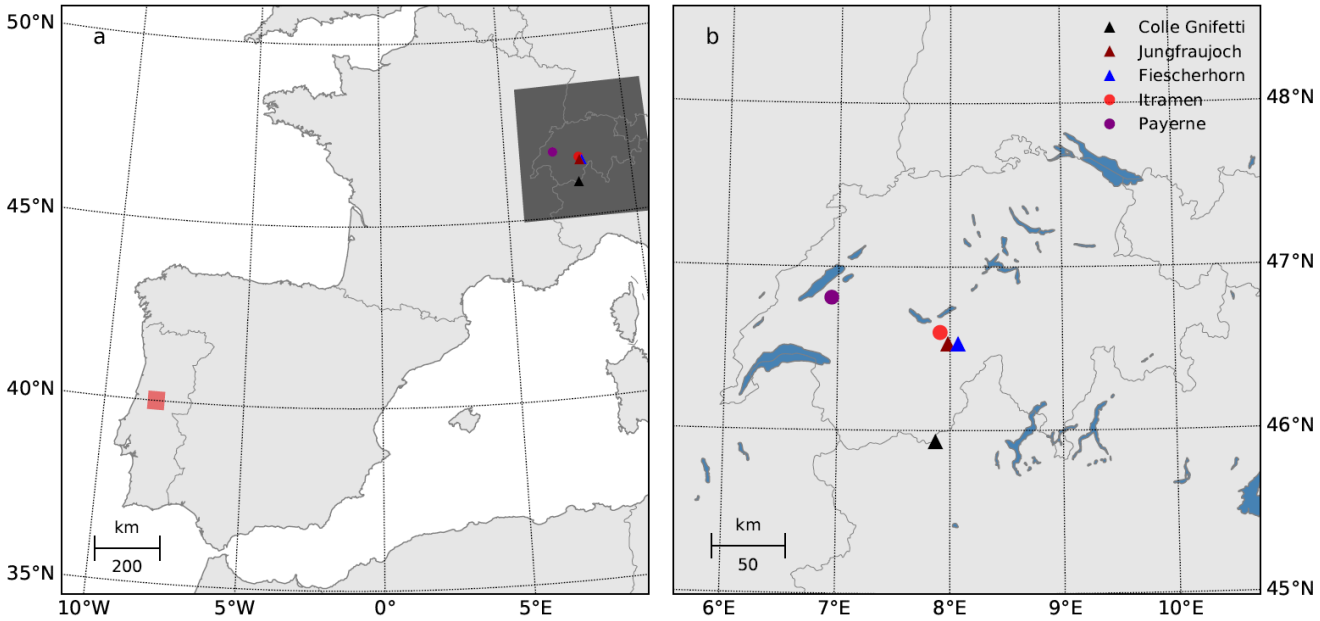

Figure 1: Source and deposition sites. a) Map of South-Western Europe with the area of Pedrógão Grande, in Central Portugal, where the fires burned (red box) and the area of the zoom in on the right panel (grey box). b) Map of Switzerland with the sites of interest mentioned in the study. Triangles indicate high-altitude ice-core and snow study sites, circles stand for weather stations.

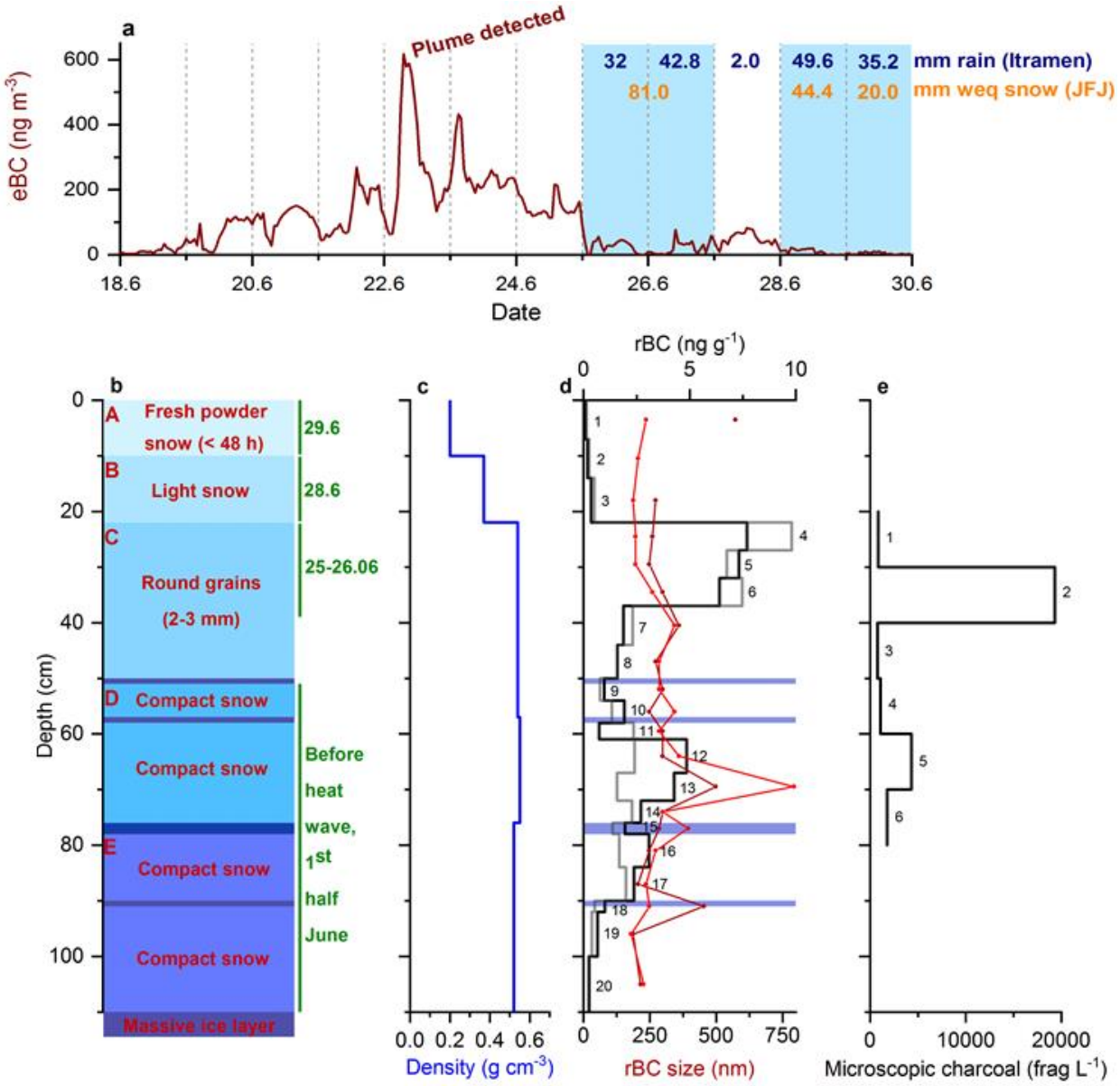

Figure 2: a) Atmospheric equivalent black carbon (eBC) concentrations at Jungfraujoch showing the peak on 22nd June when the plume of smoke reached the site. A mass absorption coefficient of 10 m^2 g^{-1} was assumed. Blue bars indicate days with significant snowfall at JFJ, with a comparison between the daily precipitation amount measured at Itramen (values in blue, in mm, data from SLF © 2019, SLF) and the daily snowfall height inferred from the snowpit at JFJ, corrected for density (values in orange, in mm water equivalent (weq)). b) Snowpit stratigraphy with ice lenses in dark blue. c) Density profile of the snowpit. d) rBC concentration profile (top scale) with the two series of replicates (black and grey) and sample number associated. Mode of the rBC mass size distribution (bottom scale) with the two series of replicates (dark red and red). Blue bars are ice lenses. e) Microscopic charcoal concentration record.

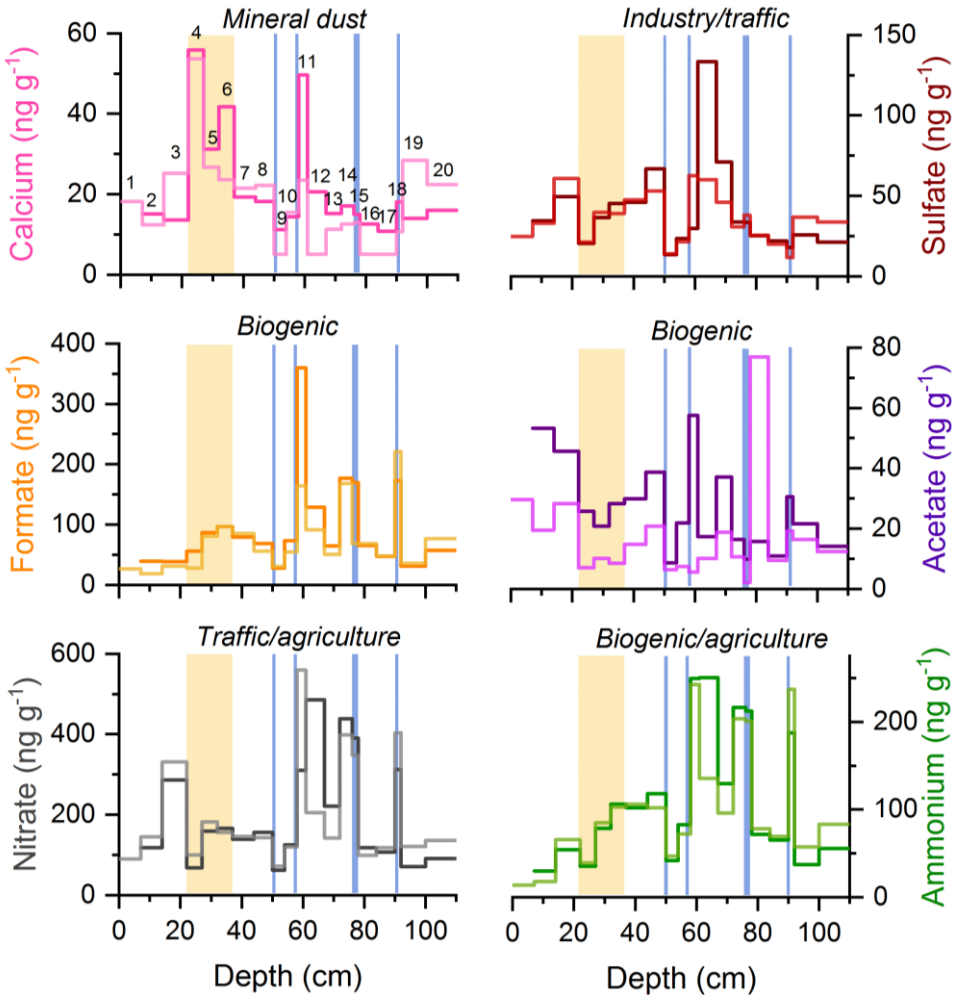

Figure 3: Ionic records from the Jungfraujoch snowpit with the two sets of replicates (darker/lighter lines). The orange bar indicates the depth at which rBC and microscopic charcoal peaks are observed. Blue bars represent ice layers. Sample numbers are specified for calcium and are similar for the other ions. Potential sources are indicated above each graph.

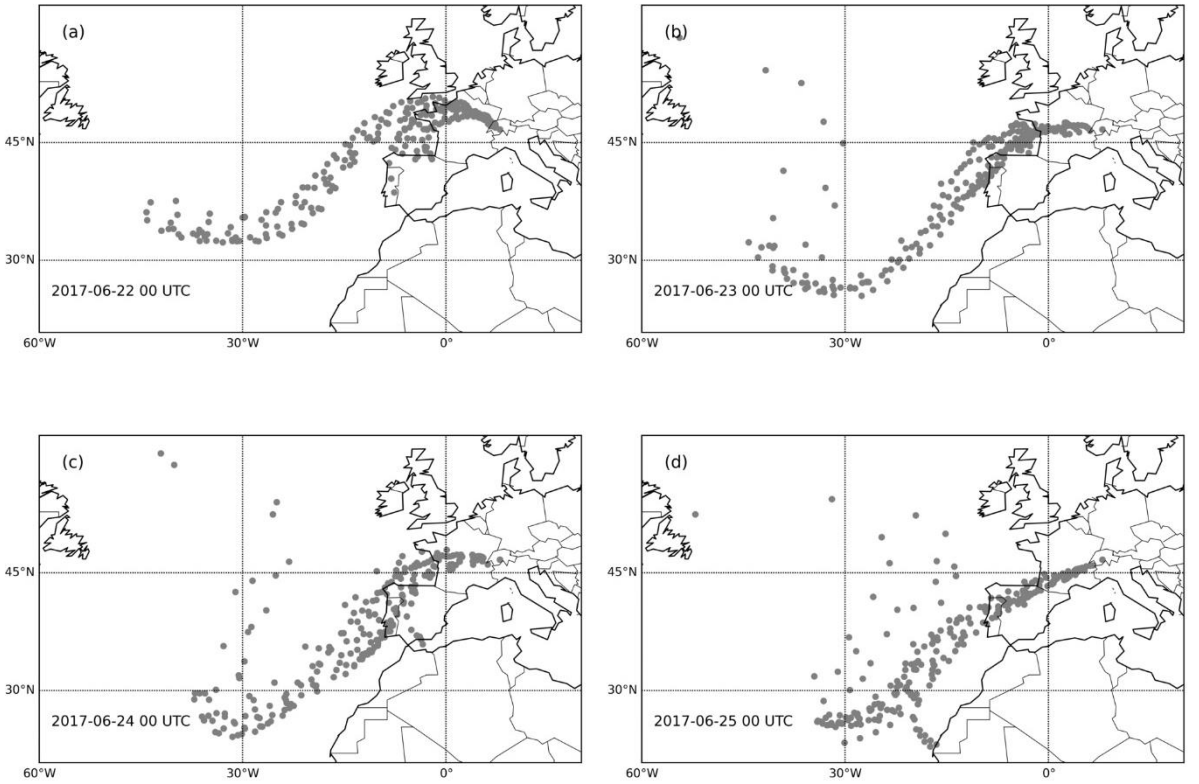
(a)
45°N
30°N
2017-06-22 00 UTC
60°W
30°W
0°
(b)
45°N
30°N
2017-06-23 00 UTC
60°W
30°W
0°
(c)
45°N
30°N
2017-06-24 00 UTC
60°W
30°W
0°
(d)
45°N
30°N
2017-06-25 00 UTC
60°W
30°W
0°

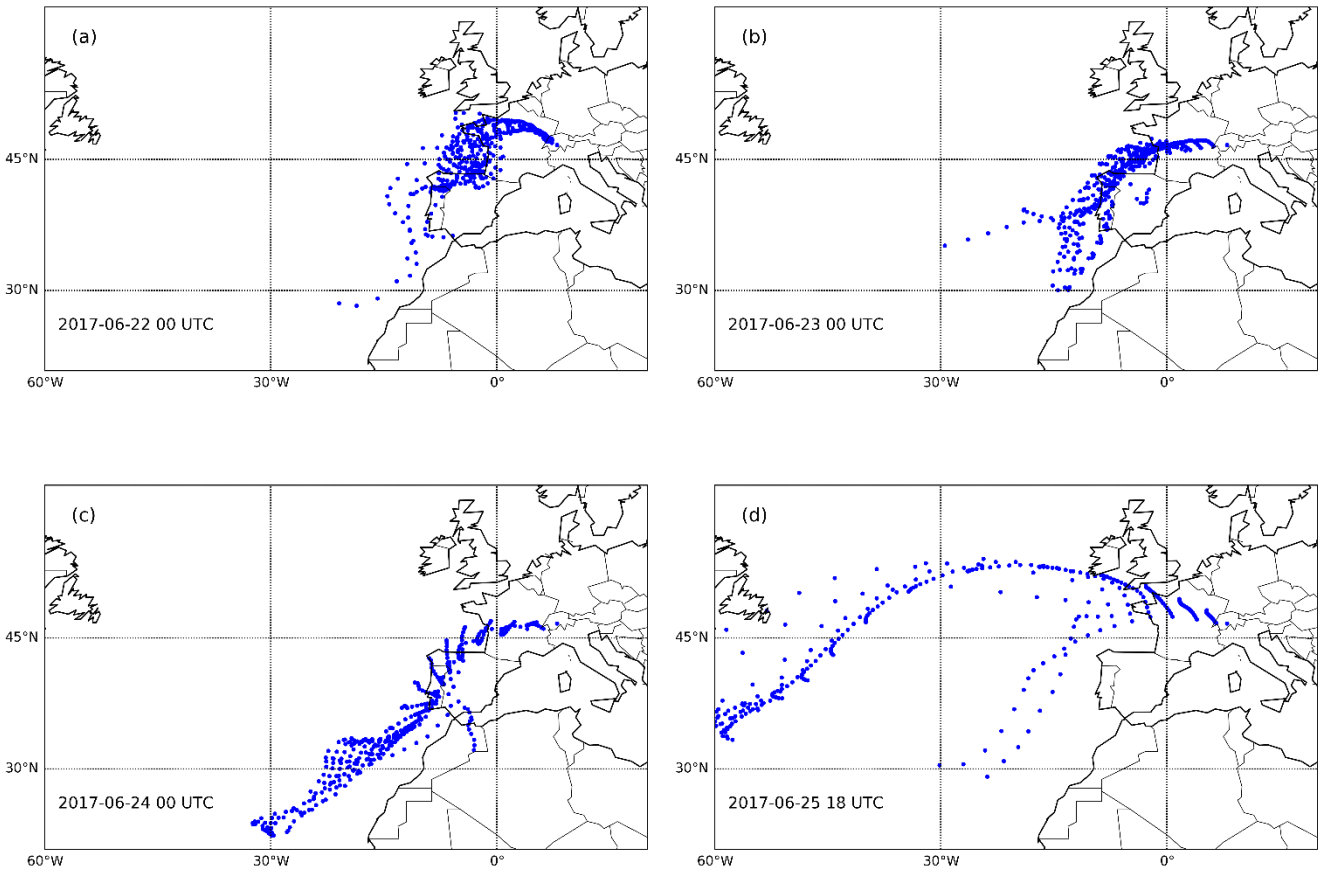

685

Figure 4: ~~35~~-day air mass backward trajectories starting ~~at~~ from the Jungfraujoch site at 00 UTC on~~for~~ ~~June~~ 22nd to 24th ~~June~~ ~~the 22nd to the 25th June~~ 2017. For ~~June~~ 25th June starting time is 18 UTC.

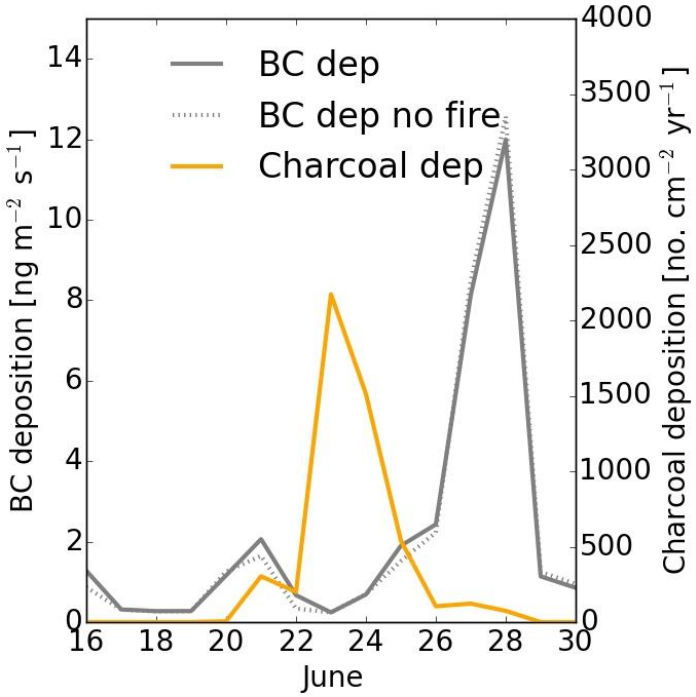

Figure 5: Simulated deposition fluxes of BC and microscopic charcoal at Jungfraujoch. In line with the observations, the deposition (dep) fluxes for BC are given as mass fluxes, whereas the deposition fluxes of microscopic charcoal are given as the number fluxes of particles larger than a certain threshold (10 µm major axis). For BC, a simulation without fire emissions (dotted gray line) and a simulation including the fire emissions near Pedrógão Grande in Central Portugal (solid gray line) are shown. For microscopic charcoal, only the simulation including fire emissions (solid orange line) is shown since biomass burning is the only source of microscopic charcoal.

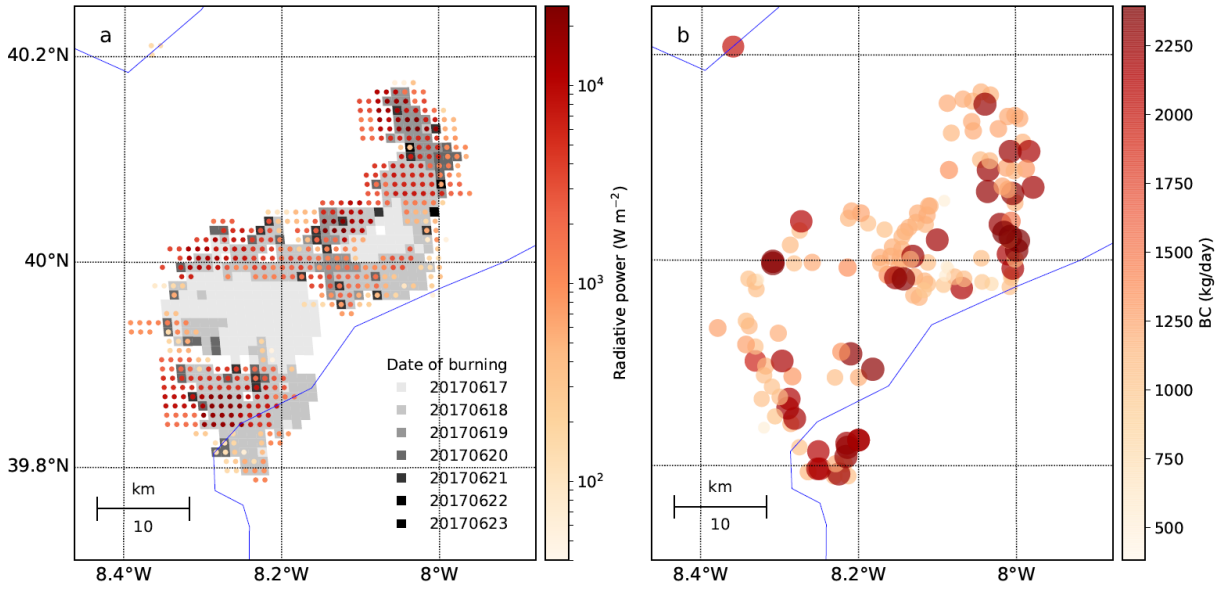

Figure 6: Spatial and temporal observed wild fires and their BC emissions near Pedrógão Grande, Portugal, for the 17th to 23th of June at 1km spatial resolution. a) Date of the area burned (MCD64A1) and maximum Fire Radiative Power (FRP) values of the active fires according to MOD14A1/MYD14A1 showing the evolved two fire clusters. b) Corresponding BC emission values based on the FINN v1.6 database with high values at the outer edges.

Author's response to referee comments on

"Tracing devastating fires in Portugal to a snow archive in the Swiss Alps: a case study", by Dimitri Osmont et al., submitted to TC

We would like to thank the referees, Paulo Fernandes and the editor for the time spent on our manuscript and for the detailed and constructive comments which helped us to improve the quality of this paper. Please find below our responses to their comments (in blue) and our changes to the manuscript (in grey and italic).

Anonymous Referee #1

Received and published: 11 March 2020

Osmont et al.

This manuscript describes a very interesting study attempting to make quantitative connection between emissions of BC, charcoal, and ionic species by fires burning in Portugal from 17 to 24 June 2017 and their deposition to snow near Jungfraujoch (JFJ) in the Bernese Alps. The case for charcoal is compelling, while the findings for BC and ionic tracers of smoke are not so clear.

A combination of remote sensing and in-situ atmospheric sampling, plus back trajectory and chemical transport modeling do show that smoke from the subject fires was transported to JFJ and was observed in the atmosphere above the snowpit site from 22 through 24 June. Atmospheric concentrations of BC dropped sharply on 25 June, coincident with significant snowfall at JFJ, and remained low until the end of June. Detailed stratigraphy and sampling for chemical analysis in a 1 m deep snow pit showed that layers representing 3 different snow events (on 25-26, 28, and 29 June) were present in the top 40 cm of the pit. Concentrations of BC were modestly enhanced and the abundance of charcoal fragments hugely increased in the layer from the first snowfall (25-26 June), but none of the ions often suggested to be smoke tracers (formate, ammonium, potassium, acetate, nitrate) were elevated. It should be noted that BC and the ions were measured in the same samples that were nominally 5 cm depth resolution while charcoal fragments were quantified in samples collected at 10 cm resolution; the BC signal in the pit appeared in 3 samples between _22 and 38 cm depth while enhanced charcoal was in a single sample covering the 30 to 40 cm depth range. It is unfortunate that the different records are not all at the same depth resolution, but the fact that the sample with peak charcoal contained some fraction of "older" snow than the deepest of the samples with elevated BC becomes important when the model results are considered. It is not possible to say from the information provided in the manuscript whether the snow between 38 and 40 cm just fell early in the event on 25 June, or included snow that had fallen days earlier, but the model suggests that much of the charcoal deposition occurred during 23-24 June compared to peak deposition of BC on the 27th and 28th.

The model also suggests that the BC peak is not due to smoke, rather it just reflects efficient scavenging of regional pollution by snow falling mainly on 27 and 28 June. The pit stratigraphy suggests that most of the BC is in snow that fell on 25-26 June, but there is some ambiguity in depth to age conversions. The authors suggest that coarse spatial resolution of the model prevents it from accurately capturing the fire emitted BC on top of a

large regional background. That may be partially true as suggested by the fact that it did not actually snow at JFJ on the 27th and only a small amount of rain was observed at the nearest weather station. However I find the performance of the model to be surprisingly good, and urge the authors to consider the possibility that while the charcoal is doubtless dominated by smoke from Portugal, the BC may be essentially just a mix of European pollution. I will first outline evidence that the model is closely reproducing the observed deposition of both BC and charcoal, and then suggest some ways the authors might be able to convince me, and other readers, that the BC is actually dominated by deposition from the smoke plume.

In section 3.6 the authors suggest that the CTM underestimates charcoal deposition by about a factor of 20 and that of BC by two orders of magnitude. It is not entirely clear how the fluxes were estimated from the observations in the snow pit since there is some ambiguity regarding the proper timescale, but here is a straightforward approach that suggests much better agreement.

The charcoal sample # 2 contains 20,000 fragments/L of snow or 20 fragments/g. The density of 0.54 g snow/cmˆ3 times the depth of the sample indicates that the 30-40 cm layer contains 5.4 g snow/cmˆ2, when multiplied by 20 fragments/g this indicates that 108 fragments/cmˆ2 were deposited (total for the event, not per second, day or year). From Fig 5 I estimate that the model deposited this on 23, 24, and 25 June at rates of 2200, 1500, and 600 fragments/cmˆ2 y, respectively. Using simple average of 14,333 fragments/cmˆ2 y x 1/365 d/year x 3 days gives modeled deposition of 118 fragments/cmˆ2 which is almost too close to 108 to be possible, given concerns about the model and especially the emissions of charcoal by the fire (scaled to BC estimates from a completely different model).

We appreciate the careful reconsidering of the fluxes and agree with the reviewer that the approach of calculating total fluxes is more straightforward, circumventing the uncertainty in the time scales. However, the reviewer used a wrong average value for the charcoal concentrations (14333 instead of 1433). We get an integral charcoal flux of 13.8 fragments cm^{-2} from the model, compared to a measured total charcoal flux of 104 fragments cm^{-2}, which is still a factor of 8 underestimation by the model.

Similar calculation for BC starts with estimate of 7.5 ng/g (average of the 6 samples #s 4-6, all replicated, in Fig 2) x 0.54 g/cmˆ3 x 15 cm (depth of the 3 samples combined) yielding total burden of 61 ng BC/cmˆ2 in this layer. For the model estimate an eyeball average of the calculated flux over 26-28 June is 6 ng/mˆ2 sec x 3 d x 86,400 sec/d x 1/10,000 cmˆ2/mˆ2 = 155 ng BC/cmˆ2. Not as close as the agreement between observed and modeled charcoal deposition but a factor of 2.5 is nowhere near 100-fold difference.

The measured total BC flux of 61 ng cm^{-2} is correct and the modelled integral flux is 195 ng cm^{-2}, so the model overestimates the flux by a factor of 3. Interestingly, the model underestimates the charcoal and overestimates the BC flux. When the model performance was evaluated with longer-term charcoal deposition fluxes, the opposite was observed (Gilgen et al., 2018). It was hypothesized that the model overestimates the fluxes at ice core sites because of their high location within complex topography. The model is not able to simulate these high locations correctly since the surface altitude is constant over the whole grid box; i.e. the topography is smoothed. In addition, ice cores are often located above the top plume height of most fires (Rémy et al., 2017), which may prevent transport of charcoal particles to them. Obviously the Pedrógão Grande case was exceptional, since the plume

was transported at elevations between 3000 and 5000 m a.s.l.. In addition, an underestimation of the fire emissions might have played a role. In contrast, the smoothed topography in the model and the corresponding more efficient vertical mixing might have resulted in overestimated levels of BC from regional anthropogenic sources, explaining the overestimation of the BC flux. We revised the manuscript accordingly:

L323-328: For microscopic charcoal, we observed a total deposition flux of 104 fragments cm^{-2} in the snowpit, around 8 times more than the modelled flux of 13.8 fragments cm^{-2} (integral over 23rd and 24th June, Fig. 5). Compared to yearly average fluxes from high-alpine ice archives (Table 4), the estimated influx at JFJ during the event is exceptional and cannot be explained by the somewhat lower altitude of the JFJ site compared to the other alpine ice-core locations. The comparison with other ice archives suggests this single outstanding event deposited nearly as many charcoal particles as during an average year in other ice archives (e.g. Brugger et al. 2018a).

L329-342: For rBC, the total deposition flux for samples 4, 5, and 6 was 62 ng cm^{-2} (average of replicate samples). The integral flux retrieved from the model for 26th, 27th, and 28th June is 195 ng cm^{-2} (Fig. 5); a factor of three higher than the observation. Interestingly, the model underestimates the charcoal and overestimates the BC flux. When the model performance was evaluated with longer-term charcoal deposition fluxes, the opposite was observed (Gilgen et al., 2018). It was hypothesized that the model overestimates the fluxes at ice core sites because of their high location within complex topography. The model is not able to simulate these high locations correctly, since the surface altitude is constant over the whole grid box; i.e. the topography is smoothed. In addition, ice core sites are often located above the top plume height of most fires (Rémy et al., 2017), which may prevent transport of charcoal particles to them. Obviously the Pedrógão Grande case was exceptional, since the plume was transported at elevations between 3000 and 5000 m a.s.l.. In addition, an underestimation of the fire emissions might have played a role for the charcoal flux. Contrary to the effect on charcoal, the smoothed topography in the model and the corresponding more efficient vertical mixing might have resulted in overestimated levels of BC from regional anthropogenic sources, explaining the overestimation of the BC flux.

To me, this suggests that the scenario suggested by the model is plausible even if not precisely correct in detail. Passage of smoke over JFJ caused dry deposition of char-coal sometime (hours or maybe a few days) before it started snowing on 25 June. Very little BC or ionic smoke tracers were removed by this process. Then a change in transport just before or coincident with the snow fall event brought air with regional pollution but very little or no smoke from Portugal to JFJ. Wet deposition via the snow created an anthropogenic BC enhancement that lacks any formate, ammonium, potassium, etc.

This is a really helpful suggestion, and the point was raised also by referee 2. We were from the beginning puzzled by not finding elevated concentrations of the other fire tracers (ammonium, formate, and acetate) in the samples 4-6. Re-considering this in view of both referee's comments, we revised our interpretation. Charcoal originating from the Portugal fires was deposited by dry deposition during the period 22nd-24th June, when the fire plume was detected by atmospheric eBC measurements at JFJ. Since no snowfall occurred during that period, the majority of BC was not deposited, since dry deposition is not efficient for submicron particles. Dry deposition of charcoal most likely resulted in a confined layer, which was not resolved with the 10 cm sampling resolution. With the snowfall on 25th June,

air mass transport changed, ending the advection of the fire plume to the JFJ as indicated by the backward trajectories arriving at JFJ at 18 UTC (will be included in Fig. 4 in the revised version). Instead more regional polluted air masses were scavenged. That the charcoal and rBC peaks partly overlap is most likely due to the coarse resolution of the charcoal samples. The change of air masses does explain the lack of a peak in the other fire tracers, e.g. ammonium, and the time delay between the charcoal and the BC peak in the model output and the snow pit data. The manuscript was changed accordingly.

Abstract:

L26-38: According to modelled emissions of the FINN v1.6 database, the fire emitted a total amount of 203.5 tons BC from a total burned area of 501 km^2 as observed on the basis of satellite fire products. Backward trajectories unambiguously linked a peak of atmospheric equivalent BC observed at the Jungfraujoch research station on 22nd June, with elevated levels until the 25th June, with the highly intensive fires in Portugal. The atmospheric signal is in correspondence with an outstanding peak in microscopic charcoal observed in the snow layer, depositing nearly as many charcoal particles as during an average year in other ice archives. In contrast to charcoal, the amount of atmospheric BC deposited during the fire episode was minor due to a lack of precipitation. Simulations with a global aerosol climate model supported that the observed microscopic charcoal particles originated from the fires in Portugal and that their contribution to the BC signal in snow was negligible. Our study revealed that microscopic charcoal can be transported over long distances (1500 km), and that snow and ice archives are much more sensitive to distant events than sedimentary archives, for which the signal is dominated by local fires. The findings are important for future ice-core studies, as they document that for BC as fire tracer the signal preservation depends on precipitation. Single events, like this example, might not be preserved due to unfavorable meteorological conditions.

Fire tracers:

L237-241: We hypothesize that charcoal originating from the Portugal fires was deposited by dry deposition during the period 22nd to 24th June, when the fire plume arrived at the JFJ as detected by elevated atmospheric eBC concentrations. Since no snowfall occurred during that period, the majority of BC was not deposited. Dry deposition most likely resulted in a confined charcoal layer, which was not separated from the rBC peak in the snowpit due to the coarse sampling resolution of 10 cm. With the beginning of snowfall on 25th June, air mass transport changed, ending the advection of the fire plume to the JFJ as indicated by backward trajectories (see below and Fig. 4). Instead more regional polluted air masses were scavenged, which explains the absence of ionic fire tracers and of a shift in the rBC size distribution.

Atmospheric transport:

L271-274: The back trajectories with arrival at JFJ on 25th June at 18 UTC indicate a major change in the synoptic situation to more north-westerly flow directions. We can only speculate that this happened concomitant with the onset of precipitation, since the timing of the latter is not precisely known.

L279-283: Furthermore, other BC sources than fires seem to dominate in our simulations, which is in agreement with our hypothesis that during fire plume arrival at JFJ the majority of fire-related BC was not deposited due to the lack of snowfall. With the beginning of

snowfall at JFJ, air mass transport changed and more regional polluted air masses with minor or without fire contribution were scavenged.

Conclusions:

L349-350: Dry deposition of microscopic charcoal resulted in an outstanding peak in the snowpack. This event deposited nearly as many charcoal particles as during an average year in other ice archives.

L354-363: For rBC, in contrast, concentrations in the snow were not exceptionally high. In combination with the absence of a peak in ionic fire tracers such as ammonium, this suggest that the majority of atmospheric BC was not deposited during the fire episode due to a lack of precipitation. Instead the observed rBC peak was mostly likely caused by scavenging of air masses containing regional pollution with the beginning of snowfall on 25th June, which ended the advection of the fire plume to the JFJ. rBC scavenging ratios were in line with previous studies, giving additional evidence that rBC was predominantly scavenged by wet deposition. Simulations with a global aerosol climate model supported that the observed microscopic charcoal particles originated from the fires in Portugal, whereas their contribution to the BC signal in snow was minor. The findings of our case study are important for future ice-core studies, as they document that for BC as fire tracer the signal preservation depends on precipitation and wet deposition. Single events, like this example, might not be preserved due to the unfavorable meteorological conditions.

Using a regional CTM with grid size in the 4-10 km range rather than the global version selected initially might help to clarify whether the BC is linked to the fires rather than being mostly regional pollution. A simpler/cheaper, but also complementary, approach would be to run forward trajectories from the fire, possibly over the entire 17-24 June lifetime but at least beginning early enough to capture the first time smoke reaches JFJ on 22 June and continuing until the fire is out. In the scenario laid out in the manuscript these trajectories would have to show strong connection between the fire and JFJ lasting well into 25 June, while the alternative outlined above predicts that the smoke clears out over JFJ before it starts snowing.

We calculated forward trajectories as suggested by the reviewer and they basically agree with the backward trajectories. We prefer to keep the backward trajectories in the manuscript, since they are more conclusive, but added the one arriving at JFJ on 25th June 18 UTC to show the change to north-westerly air flow. We show now trajectories calculated 5-days backward at 20 equidistant levels in pressure coordinates between 700 hPa and 500 hPa, in accordance with the detected smoke plume height.

To the best of our knowledge, the ECHAM-HAM is the only model with a charcoal module implemented. We included that in the manuscript.

Figure 4.

L142-143: To the best of our knowledge, this is the only model with a charcoal module implemented.

As noted right at the beginning, this is an interesting story, and the firm results for charcoal make it important to get before the community. I think that the argument linking the BC in the snow to the fires needs to be made much more convincingly, or ruled out just as

strongly. Neither option would impact the charcoal connection, while insisting that the BC is fire derived based on weak evidence lessens the power of the manuscript.

See comment above.

Following are a list of specific comments and editorial suggestions, keyed to line number.

27 As noted above, the correspondence between eBc measured through 24 June and rBc measured in snow that fell 25-26 June may be more tenuous than asserted.

Agreed, see comment above.

28-29 Calculated scavenging ratios may be oversold since there is no assurance that BC at cloud height 25 and 26 June was same as inferred from measured eBc on the ground 24 June.

We agree with that comment, but this is the case for most of the published scavenging ratios. Since there are so few data we decided to keep it.

33-34 "This study unambiguously links charcoal in the snow with the highly intensive fires in Portugal: : :" At least one reader is not convinced that rBC in the snow is from these fires, and would liked to have seen some of the ionic tracers supporting that inference yet none do.

Agreed, see above. The sentence was deleted.

35 Is the BC emission estimate not basically straight from FINN, rather than ECHAM?

Thanks for noticing. Yes, the accumulated amount of 203.5 tons BC is based on modelled emissions on the FINN v1.6 database (see also 305). We have rewritten the sentence as in the following:

L26-27: According to modelled emissions of the FINN v1.6 database, the fire emitted a total amount of 203.5 tons BC.

39 what do you mean by "landscape" fires, as something distinct from biomass fires

Bowmann et al. (2009) distinguish between "landscape" fires, "biomass combustion for domestic and industrial uses, and fossil-fuel combustion". Thus, "including landscape and biomass" refers to landscape fires and biomass combustion for domestic and industrial uses. We have clarified this accordingly.

L41-43: Global CO_2 emissions from fires, including landscape and biomass (i.e. biomass combustion from domestic and industrial uses), represent around 50% of those produced by fossil fuel burning (Bowmann et al., 2009).

50 consider citing some of the pioneering studies of fire tracers in polar ice cores, for example; Legrand et al., 1992 (GRL); Whitlow et al., 1994 (Tellus; Legrand and De Angelis, 1996 (JGR)

Are now included (L53).

92-94 Sentence pointing out that ice cores from near JFJ have been studied is not needed unless you later make some connection to the cited papers.

The sentence was deleted.

97 located on the eponymous pass between—! located between

OK, eponymous was deleted.

135-138 Might want to state the dates for which backtrajectories were calculated. And as noted above, consider running forward trajectories from the fire as well.

Was included in the caption of Figure 4. Forward trajectories were calculated, see above.

Figure 4: 5-day air mass backward trajectories starting from the Jungfraujoch site at 00 UTC on 22nd to 24th June 2017. For 25th June starting time is 18 UTC.

139-149 If you cannot, or decide not to, run a regional model, I think you should provide more justification for choosing to run this particular version of ECHAM, especially since you kind of denigrate its performance later in the manuscript.

To the best of our knowledge, the ECHAM-HAM is the only model with a charcoal module implemented.

L142-143: To the best of our knowledge, this is the only model with a charcoal module implemented.

151-157 Curious why you chose to only use MODIS products. It is becoming increasingly clear that important details are missed due to coarse spatial resolution, and the fixed single overpass time. Are there not relevant products from the Sentinel satellites? Geostationary platforms (mainly supporting meteorology forecasting) can provide insight throughout the day, especially later in the afternoon when many fires are strongest.

We analysed higher spatial resolution Soumi/VIIRS active fire products (375m) next to MODIS active fire products to obtain a better understanding on the spread and evolution of the fire (see also answer to the comment of Paulo Fernandes). To be consistent with the emission estimates of the FINN v1.6 database (based on MODIS active fire data), we decided here to show MODIS fire products. To make this clearer we rephrased it in the manuscript.

L157-159: In consistency with FINN v1.6, we chose the Thermal Anomalies & Fire Daily L3 Global Product, which is also utilized for the emission model. In addition, we obtained the Burned Area Monthly L3 Global Product of MODIS.

184 I would not say that peak rBC of 9.8 ng/g is “remarkable”. It is only about 2 x higher than the secondary peak at 60-70 cm depth. The Thomas et al., 2017 paper cited elsewhere found the average peak in 22 north Greenland pits to be 15 ng/g, with max of 43 ng/g with longer transport distances back to the source fires.

Agreed, remarkable was deleted.

193-194 I would mention the secondary rBC peak in samples 12/13 that overlaps the bump up in charcoal sample 5, especially since you point out the increased size later to suggest more local source.

Good point. We now mention this secondary rBC peak.

L197-200: Below the rBC peak, a secondary rBC maximum with 4.5 ng g^{-1} was observed between 60 and 70 cm in one replicate series, but otherwise average concentrations are low (2.0 ng g^{-1}). Except for this secondary maximum, a very good agreement is obtained between the two series of replicate rBC samples (r = 0.90, all samples).

197 Regarding the “narrower” charcoal peak, I think it may mostly be in the 2 cm interval 28-30 cm below rBC sample 6, but that is just a hypothesis.

That seems likely, but we cannot proof it with our data. We added this sentence.

L239-240: Dry deposition most likely resulted in a confined charcoal layer, which was not separated from the rBC peak in the snowpit due to the coarse sampling resolution of 10 cm.

270-280 As noted above, consider forward trajectories from the fires, specifically looking to see if smoke was likely over JFJ when it started snowing 25 June. And seriously consider whether ECHAM is possibly correct that the BC in the snow is not from the fires.

See comment above.

Section 3.5 See earlier question about exclusive reliance on MODIS, and the on-line comment from Paolo Fernandes.

See above reason for using MODIS and our response to the comment from Paolo Fernandes.

Section 3.6 Consider the "deposited" BC and charcoal calculations presented in introductory comments. If you decide to stick with flux estimates provide more details about assumptions used to get values so much higher than the model.

Calculations were changed, see comment above.

Last paragraph of this section, seems that the model thought there was no smoke at all over JFJ, pointing to a transport shift (or error) rather than problems with emissions. I made a case that the model came within factor of 2.5 of the total amount of BC in the snow from 25-26 June, even though it wants to deposit most of it on the 27th and 28th . Might be worth comparing the timing and amount of precipitation in the model to observations.

We extracted only deposition from the model. Since the model obtained the charcoal deposition peak, it must have seen the smoke over JFJ. See also our above comment on the fluxes.

Anonymous Referee #2

Received and published: 6 April 2020

This manuscript attempts to link emissions from a known fire event and their deposition on snow close to JFJ in the Swiss Alps through extensively investigating a severe fire event occurred on 17-24 June 2017 in Portugal. This study is attempting to provide an interesting approach, connecting a set of valuable record of charcoal, black carbon, and ions in the snow pit and a combination of atmospheric in-situ measurement, remote sensing, air mass trajectory calculation, and transport simulation, to better understand the information of particle deposition in snow in European high-altitude sites. This approach is very useful to understand atmospheric processes of aerosol particles how to transport over long distances, be scavenged by snow fall, and be deposited to snow by providing clues. However, there is an issue that should be considered seriously to publish the results. Authors measured charcoal, refractory black carbon (rBC), and ions in snow collected near JFJ and compared their profiles with equivalent black carbon (eBC) measured in the atmosphere at JFJ. The elevations of charcoal in the upper layer of C in snow (sample "2" in figure 2e) and eBC in atmosphere on 22 June (figure 2a) were obvious with an increase relative to background level by _6 times and _10 times, respectively, indicating that the fire plume reached JFJ. In contrast to them, rBC in sample "4-6" (figure 2d) increased a little and changes in ion concentrations are even indiscernible. Readers reasonably expect that potassium,

ammonium, and nitrate can be elevated in their concentrations if the big fire plume indeed reached and is detectable by charcoal and eBC. In the same snow layer, the rBC concentration was elevated just 1.5 times relative to the second peak with rBC concentration of _5 ng/g, that is probably from local fires as suggested by authors. Discuss this issue in dept and provide more evidences and/or assumption to support your argument.

This is a really helpful suggestion, and the point was raised also by referee 1. We were from the beginning puzzled by not finding elevated concentrations of the other fire tracers (ammonium, formate, and acetate) in the samples 4-6. Re-considering this in view of both referee's comments, we revised our interpretation. Charcoal originating from the Portugal fires was deposited by dry deposition during the period 22nd-24th June, when the fire plume was detected by atmospheric eBC measurements at JFJ. Since no snowfall occurred during that period, the majority of BC was not deposited, since dry deposition is not efficient for submicron particles. Dry deposition of charcoal most likely resulted in a confined layer, which was not resolved with the 10 cm sampling resolution. With the snowfall on 25th June, air mass transport changed, ending the advection of the fire plume to the JFJ as indicated by the backward trajectories arriving at JFJ at 18 UTC (will be included in Fig. 4 in the revised version). Instead more regional polluted air masses were scavenged. That the charcoal and rBC peaks partly overlap is most likely due to the coarse resolution of the charcoal samples. The change of air masses does explain the lack of a peak in the other fire tracers, e.g. ammonium, and the time delay between the charcoal and the BC peak in the model output and the snow pit data. The manuscript was changed accordingly.

Abstract:

L26-38: According to modelled emissions of the FINN v1.6 database, the fire emitted a total amount of 203.5 tons BC from a total burned area of 501 km^2 as observed on the basis of satellite fire products. Backward trajectories unambiguously linked a peak of atmospheric equivalent BC observed at the Jungfraujoch research station on 22nd June, with elevated levels until the 25th June, with the highly intensive fires in Portugal. The atmospheric signal is in correspondence with an outstanding peak in microscopic charcoal observed in the snow layer, depositing nearly as many charcoal particles as during an average year in other ice archives. In contrast to charcoal, the amount of atmospheric BC deposited during the fire episode was minor due to a lack of precipitation. Simulations with a global aerosol climate model supported that the observed microscopic charcoal particles originated from the fires in Portugal and that their contribution to the BC signal in snow was negligible. Our study revealed that microscopic charcoal can be transported over long distances (1500 km), and that snow and ice archives are much more sensitive to distant events than sedimentary archives, for which the signal is dominated by local fires. The findings are important for future ice-core studies, as they document that for BC as fire tracer the signal preservation depends on precipitation. Single events, like this example, might not be preserved due to unfavorable meteorological conditions.

Fire tracers:

L237-241: We hypothesize that charcoal originating from the Portugal fires was deposited by dry deposition during the period 22nd to 24th June, when the fire plume arrived at the JFJ as detected by elevated atmospheric eBC concentrations. Since no snowfall occurred during that period, the majority of BC was not deposited. Dry deposition most likely resulted in a confined charcoal layer, which was not separated from the rBC peak in the snowpit due to

the coarse sampling resolution of 10 cm. With the beginning of snowfall on 25th June, air mass transport changed, ending the advection of the fire plume to the JFJ as indicated by backward trajectories (see below and Fig. 4). Instead more regional polluted air masses were scavenged, which explains the absence of ionic fire tracers and of a shift in the rBC size distribution.

Atmospheric transport:

L271-274: The back trajectories with arrival at JFJ on 25th June at 18 UTC indicates a major change in the synoptic situation to more north-westerly flow directions. We can only speculate that this happened concomitant with the onset of precipitation, since the timing of the latter is not precisely known.

L279-283: Furthermore, other BC sources than fires seem to dominate in our simulations, which is in agreement with our hypothesis that during fire plume arrival at JFJ the majority of fire-related BC was not deposited due to the lack of snowfall. With the beginning of snowfall at JFJ, air mass transport changed and more regional polluted air masses with minor or without fire contribution were scavenged.

Conclusions:

L349-350: Dry deposition of microscopic charcoal resulted in an outstanding peak in the snowpack. This event deposited nearly as many charcoal particles as during an average year in other ice archives.

L354-363: For rBC, in contrast, concentrations in the snow were not exceptionally high. In combination with the absence of a peak in ionic fire tracers such as ammonium, this suggest that the majority of atmospheric BC was not deposited during the fire episode due to a lack of precipitation. Instead the observed rBC peak was mostly likely caused by scavenging of air masses containing regional pollution with the beginning of snowfall on 25th June, which ended the advection of the fire plume to the JFJ. rBC scavenging ratios were in line with previous studies, giving additional evidence that rBC was predominantly scavenged by wet deposition. Simulations with a global aerosol climate model supported that the observed microscopic charcoal particles originated from the fires in Portugal, whereas their contribution to the BC signal in snow was minor. The findings of our case study are important for future ice-core studies, as they document that for BC as fire tracer the signal preservation depends on precipitation and wet deposition. Single events, like this example, might not be preserved due to the unfavorable meteorological conditions.

L135: Since the fire event studied in this work was a well-documented recent extreme event, authors need to calculate forward air mass trajectories to see if the plume departing from the exact fire spot reach the JFJ site. Consider that a starting height of air mass trajectories is not necessarily just above ground because fire-emitted particles can be directly injected into the free troposphere up to > 3 km. Also, it would be great to see if the area-averaged time series of AOD match with forward air mass trajectories. For AOD, just simply check GIOVANNI platform (https://giovanni.sci.gsfc.nasa.gov/giovanni/#service=DiArAvTs&starttime=&endtime=&bbox=- 180,-90,180,90). Intense fire plumes are often easily captured by AOD, and thus AOD near JFJ should be elevated day-by day.

We calculated forward trajectories as suggested by the reviewer and they basically agree with the backward trajectories. We prefer to keep the backward trajectories in the manuscript, since they are more conclusive, but added the one arriving at JFJ on 25th June 18 UTC to show the change to north-westerly air flow. We show now trajectories calculated 5-days backward at 20 equidistant levels in pressure coordinates between 700 hPa and 500 hPa, in accordance with the detected smoke plume height.

Thanks for the suggestions of the GIOVANNI database to explore changes in AOD concentrations. We had a look into different daily AOD products (e.g. from OMAEROe v003 at 0.25° (smallest spatial resolution in the GIOVANNI database) to the MODIS-Terra MOD08_D3 v6.1. at 1° spatial resolution) and their area-averaged time series for 17th until 26th of June. However, this didn't help to address your question because 1) of their rather coarse spatial resolution, 2) cloud coverage which obscured the satellite's view. The data are inclusive because of their poor spatial resolution.

In addition, we looked at AOD data with a spatial resolution of 10 km at nadir from the Modis sensor flying onboard of the satellites Terra and Aqua, which support that between 20th and 22nd of June the JFJ site received air masses with elevated AOD concentrations from Portugal. The AOD concentration levels increased over Switzerland mainly North of the Alps during that time, in agreement with the backward trajectories (Fig. 4). From 23rd to 25th of June the area was cloud covered, so AOD could not be retrieved.

This was included in the manuscript.

L172-175: To detect the fire plume, we analyzed different daily Aerosol Optical Depth (AOD) products from OMAEROe v003 at 0.25° (smallest spatial resolution in the GIOVANNI database), MODIS-Terra MOD08_D3 v6.1. at 1° spatial resolution, and from the Modis sensor flying onboard of the satellites Terra and Aqua at a spatial resolution of 10 km at nadir and their area-averaged time series for 17th until 26th of June.

L274-277: AOD data at 10 km resolution support that between 20th and 22nd of June the JFJ site received air masses with elevated AOD from Portugal. The AOD levels increased over Switzerland mainly north of the Alps during that time, in agreement with the backward trajectories (Fig. 4). From 23rd to 25th of June the area was cloud covered, so AOD could not be retrieved.

L206: The upper size limit of BBHG is generally <300 nm, although which depends on the instrumental setting. Please check if authors mentioned "BBLG" instead of "BBHG".

Thank you for discovering this! The sentence was changed accordingly.

L209-210: The mass size distribution for the broadband low gain (BBLG) channel of the SP2 remained similar throughout the profile with 306 nm and 291 nm for the two series of replicates, respectively (Fig. 2d).

L205-214: In figure 2d, the diameter of rBC particles in sample "4-6" (figure 2d) seem similar to that of other layers except for sample "13". The size of atmospheric rBC particles generated from biomass combustion is generally larger than that from urban fossil emissions. If the rBC size is not obviously large in sample "4-6", the possible reason should be suggested, regarding for example, cloud or wet-scavenging during transport and/or scavenging by snowfall, etc.

This finding fits now better with our revised interpretation, see discussion above, and changed the discussion about the size distribution.

L211-212: Only sample 13 shows a bigger fraction of large rBC particles, in association with a small peak in rBC and charcoal concentration. On the contrary, no shift in the rBC size distribution is visible for samples 4 to 6 during the peak in rBC and charcoal concentrations.

L224: Authors mentioned that smoke particles can be lifted up to free troposphere and travel over long distance. It can be true not only for charcoal but also for rBC particles. As noted above, it should be seriously considered why rBC and ionic particles did not elevated unlike charcoal. rBC particles are small with diameters < 1 micrometer, which thus can travel longer distances, as found in previous studies so far. Also, authors may need to check if the number of particles in SP2 scattering channel ("SCLG" or "SCHG") is elevated in the snow layers. The profile of scattering particles, i.e., number concentration, might correspond to that of charcoal.

We agree. rBC particles should have been transported as well. We think that charcoal was deposited by dry deposition whereas rBC was not scavenged until 25th June due to the lack of precipitation, see comment above. We revised our interpretation accordingly, see comment above.

Charcoal particles detected microscopically had a major axis >10 µm. Such large particles are not aerosolized with the nebulizer set-up and, thus, do not enter the SP2. In addition, it is not possible to analyse insoluble scattering-only particles in aerosolized snow (or other liquid) extracts since extremely large numbers of scattering particles are produced by aerosolization and drying of the dissolved components in the solution. The numbers of such particles overwhelm any SP2 scattering signals from the insoluble components.

L230: Both ammonia (NH3) and NOx can be emitted from fires, and during the transport time in the atmosphere, ammonium nitrate (NH4NO3) and other forms of nitrate and ammonium can be formed particularly under high relative humidity via aqueous reaction. Authors should seriously consider why such inorganic ions are not sufficiently detected in the snow layer corresponding to smoke plume. Meteorological conditions, for example too dry condition in FT and/or too warm in PBL, were not favorable for the aerosol formation? Moreover, potassium has been broadly used as an indicator of biomass combustion so far. Did authors observe a peak of potassium in the snow layer?

We agree and revised our interpretation accordingly, see above.

Paulo Fernandes

pamfernand@gmail.com

Received and published: 6 March 2020

This is interesting work. Just a short comment in relation to the burned area estimate. The fire blowup, with extremely high rate of spread and pyCb formation and collapse that killed 66 people, occurred on the first day of its development. As such your 17th June burned area estimates are underestimated by one order of magnitude. According to our reconstruction (CTI 2017), resulting from the combination of various ground- and remote sensing-based information, burned area on the 1st and 2nd days was 128 and 211 km2, respectively. Thus remote sensing products did not detect fire growth nor peak FRP happening at about 19-21

h PM on the 17th, presumably because of the combination of dense smoke with thunderstorm clouds.

Thank you for your comment. We actually analysed remote sensing data for the 17th, but did not describe this in detail in the manuscript. On the 17th, the fire was early detected by Soumi/VIIRS (375m) about 13:46-13:47 UTC few kilometres from a thick cumulonimbus cloud. For Aqua/MODIS 1km data (overpass time 13:45-13:50 UTC – almost simultaneous overflight), the fire was too small to be detected. This explains why FINN has no emission entries for the 17th. This was included in the manuscript.

L298-302: An additional comparison of the Aqua/MODIS and VIIRS/NPP Active Fire Product (375 m spatial resolution; Schroeder at el., 2014) showed, that the fire was early detected by the VIIRS/NPP Fire Product at ~13:46 UTC. The fire was located few kilometres away from a thick cumulonimbus cloud. Though, the overpass time of Aqua/MODIS was almost simultaneous (i.e. 13:45-13:50 UTC), the fire was too small to be detected by the coarser spatial resolution sensor (1 km). This explains why FINN v1.6 has no emission entries for 17th June.

Response to comments from the editor

Nevertheless, I will be greatly appreciate in the revised version if the authors can give the definition of eBC and rBC at first occurrence (abstract and text), referring to a published article is not enough.

Good comment, thank you. We included the definition for both in the text, but not in the abtract.

L90-92: The term eBC is used for black carbon data derived from optical absorption methods, together with a suitable mass absorption cross-section (MAC) for the conversion of light absorption coefficient into mass concentration (Petzold et al., 2013).

L123: rBC stands for black carbon measured by incandescence methods (Petzold et al., 2013)

Also, I will add a comment in the discussion as I'm very critical about the use of the scavenging ratio.

We agree with that comment, see also our comment to referee 1. Nevertheless, despite all uncertainties included, scavenging ratios give at least some indication which components are easily taken up by snow. Since there are so few data we preferred to keep them.

Also regarding the comment on AOD by review 2, even if the comparison is not fully conclusive, I suggest to mention it in your MS. I will avoid other readers to ask themselves the same question.

This was included in the manuscript.

L172-175: To detect the fire plume, we analyzed different daily Aerosol Optical Depth (AOD) products from OMAEROe v003 at 0.25° (smallest spatial resolution in the GIOVANNI database), MODIS-Terra MOD08_D3 v6.1. at 1° spatial resolution, and from the Modis sensor flying onboard of the satellites Terra and Aqua at a spatial resolution of 10 km at nadir and their area-averaged time series for 17th until 26th of June.

L274-277: AOD data at 10 km resolution support that between 20th and 22nd of June the JFJ site received air masses with elevated AOD from Portugal. The AOD levels increased over Switzerland mainly north of the Alps during that time, in agreement with the backward trajectories (Fig. 4). From 23rd to 25th of June the area was cloud covered, so AOD could not be retrieved.

Same thing for the comment of reviewer 1 for the use of the CHAM-HAM model, Please, justify in the text why you decided to use this global model instead of a regional model.

We included that in the manuscript.

L142-143: To the best of our knowledge, this is the only model with a charcoal module implemented.